Earthquake Location, Direct, Global-Search Methods

ANTHONY LOMAX[a], ALBERTO MICHELINI[b] and ANDREW CURTIS[c]

[a]ALomax Scientific, Mouans-Sartoux, France

[b]Istituto Nazionale di Geofisica e Vulcanologia, Roma, Italy

[c]ECOSSE (Edinburgh Collaborative of Subsurface Science and Engineering), Grant Institute of GeoSciences, Kings Buildings, The University of Edinburgh, Edinburgh, United Kingdom

Article Outline

Glossary

Arrival time

The time of the first measurable energy of a seismic phase on a seismogram.

Centroid

The coordinates of the spatial or temporal average of some characteristic of an earthquake, such as surface shaking intensity or moment release.

Data space

If the data are described by a vector **d**, then the data space **D** is the set of all possible values of **d**.

Direct search

A search or inversion technique that does not explicitly use derivatives.

Earthquake early-warning

The goal of earthquake early-warning is to estimate the shaking hazard of a large earthquake at a nearby population centre or other critical site before destructive *S* and surface waves have reached the site. This requires that useful, probabilistic constraint on the location and size of an earthquake is obtained very rapidly.

Earthquake location

An earthquake location specifies a spatial position and time of occurrence for an earthquake. The location may refer to the earthquake hypocentre and corresponding origin time, a mean or centroid of some spatial or temporal characteristic of the earthquake, or another property of the earthquake that can be spatially and temporally localized. This term also refers to the process of locating an earthquake.

Epicentre

The point on the Earth's surface directly above a hypocentre.

Error

A specified variation in the value assumed by a variable. See also *uncertainty*.

Global search

A search or inversion that samples throughout the prior *pdf* of the unknown parameters.

Hypocentre

The point in three-dimensional space of initial energy release of an earthquake rupture or other seismic event.

Importance sampling

A sampling procedure that draws samples following the posterior *pdf* of an inverse, optimization or other search problem. Since these problems involve initially unknown, posterior *pdf* functions, importance sampling can only be performed approximately, usually through some adaptive or learning procedure as sampling progresses.

Inverse problem, Inversion

The problem of determining the parameters of a physical system given some data. The solution of an inverse problem requires measurements of observable quantities of the physical system, and the mathematical expression (the forward problem) that relates the parameters defining the physical system (model space) to the data (data space). In inverse problems, estimates of the unknown parameters in the model space and of their uncertainties are sought from the combination of the available information on the model parameters (prior *pdf*), the data and the forward problem.

Likelihood function

A non-normalized *pdf*.

Misfit function

A function that quantifies the disagreement between observed and calculated values of one or more quantities. See objective function.

Model space

If the model parameters are described by a vector **m**, then model space *M* is the set of all possible values of **m**.

Objective function

A function expressing the quality of any point in the model space. Inversion and optimisation procedures use an objective function to rank and select models. Usually objective functions are defined in terms of misfit functions, and for probabilistic inversion the objective function must be a *pdf* or likelihood function.

Origin time

The time of occurrence of initial energy release of an earthquake rupture or other seismic event.

Prior pdf

A *pdf* that expresses the information on the unknown parameters available before an inverse problem is solved. For an earthquake location, the prior *pdf* is often a simple function (e.g., boxcar) of three spatial dimensions and time. See also *Inverse problem*.

Probability density function - pdf

A function in one or more dimensional space **X** that (i) when integrated over some interval Δ**x** in *X* gives a probability of occurrence of any event within Δ**x**, and (ii) has unit integral over space **X**, where **X** represents a space of possible events. An earthquake location *pdf* is often a 3-dimensional probability density function over all possible spatial locations or a 4-dimensional probability density function over all possible spatial locations and times of occurrence.

Posterior pdf

A *pdf* that expresses the information about the unknown parameters available after inversion. The posterior *pdf* for an earthquake location is often a function of the three spatial dimensions and the origin time of the hypocenter parameters; this function may be complicated. See also *Inverse problem*.

Ray path

A local minimum-time path between a source and receiver of idealized, infinite frequency wave energy of a specified wave type (e.g., *P* or *S*).

Receiver or Station

Synonyms for an observation point where ground motion is detected and a seismogram recorded.

Seismic phase

A distinct packet of energy from a seismic source. Usually refers to a specified wave type (e.g. *P* or *S*) satisfying a particular physics of wave propagation.

Seismicity

The distribution in space and time of seismic event locations.

Seismogram

An analogue or digital recording of the ground motion at a point (receiver or station) in the Earth. Also called a waveform.

Source

A general term referring to an earthquake, explosion or other release of seismic energy as a physical phenomenon localized in space and time.

Station

See *receiver*.

Travel time

The time that a signal, *e.g.* elastic wave energy of a seismic phase, takes to propagate along a ray path between two points in a medium.

Uncertainty

Random variation in the values assumed by a variable. See also *error*.

I.   Definition of the Subject and Its Importance

An earthquake location specifies the place and time of occurrence of energy release from a seismic event. A location together with a measure of size forms a concise description of the most important characteristics of an earthquake. The location may refer to the earthquake's epicentre, hypocentre, or centroid, or to another observed or calculated property of the earthquake that can be spatially and temporally localized. A location is called *absolute* if it is determined or specified within a fixed, geographic coordinate system and a fixed time base (e.g., Coordinated Universal Time, UTC); a location is called *relative* if it is determined or specified with respect to another spatio-temporal object (e.g., an earthquake or explosion) which may have unknown or uncertain absolute location.

For rapid hazard assessment and emergency response, an earthquake location provides information such as the locality of potential damage or the source region of a possible tsunami, and a location is required to calculate most measures of the size of an earthquake, such as magnitude or moment. Locations are required for further analysis and characterisation of the event, for studies of general patterns of seismicity, to calculate distributions of stress and strain changes around the earthquake, for assessing future earthquake hazard, and for basic and applied seismological research.

Since earthquakes occur deep in the Earth, their source locations must be inferred indirectly from distant observations, and earthquake location is thus a remote-sensing problem. Most commonly an earthquake location is determined by the match or misfit between observed arrival times of seismic wave-energy at seismic stations, and predictions of these arrival times for different source locations using a given elastic-wave speed model; this is an inverse problem. Essentially, many potential locations (place and time) are examined and those for which some measure of misfit between predicted and measured arrival times is smallest are retained as best estimates of the true location.

Many numerical location methods involve linearization of the equations relating the predicted arrival times to the location through Taylor expansion involving partial derivatives; these are called *linearized* methods. Methods that do not are called *nonlinearized* or *direct-search* methods. The term *nonlinear* is used ambiguously in geophysics to refer to linearized-iterated and to nonlinearized methods. In this chapter we focus on nonlinearized, direct-search methods, and to avoid ambiguity we identify them with the term *direct-search*.

Direct-search location can be performed through graphical analyses, regular or stochastic searches over a space of possible locations, and other algorithms. Direct-search earthquake location is important because, relative to linearized methods, it is easy to apply with realistic earth models which may have abrupt and complicated variations in three-dimensions, it places little restriction on the form of the measure of misfit, it is stable (*i.e.*, does not suffer numerical convergence problems) when the observations are insufficient to fully constrain the spatial location or origin time, and it can produce comprehensive, probabilistic solutions which indicate the full location uncertainty, often a complex functions of space and time. Conversely, the primary advantage of linearized location methods is that they are much less demanding computationally than direct-search methods.

II.   Introduction

Most commonly, an earthquake location is determined using observed seismic-phase arrival-times and associated uncertainties, and predicted travel times in a given wave-speed model. Ideally, the location procedure will determine a 4-dimensional, posterior probability density function, or location *pdf*, over all possible solutions (spatial locations and origin times). This location *pdf* quantifies the agreement between predicted and observed arrival times in relation to all uncertainties, and forms a complete, probabilistic solution. In practice, however, an earthquake location is often specified as some optimal solution (a point in space and time) with associated uncertainties.

The earliest, formal earthquake locations using seismic-phase arrival-time observations employed direct-search procedures such as graphical methods (*e.g.*, Milne, 1886) or simple grid searches (*e.g.*, Reid, 1910). The advent of digital computers in the 1960's lead to the use of iterated linearized approaches based mainly on Geiger's method (1912). Since the 1980's, the increasing power of digital computers has made large-scale, grid and stochastic direct searches practical for routine earthquake location. Direct-search methods are now used routinely in research and earthquake monitoring (*e.g.*, Sambridge and Kennett, 1986; Johnson *et al.*, 1994; Rabinowitz, 2000; Husen *et al.*, 2003; Husen and Smith, 2004; Presti *et al.*, 2004; Lomax, 2005; Horiuchi *et al.*, 2005; Lomax, 2008).

In principle, direct-search methods can be applied to locate the relative positions of ensembles of events, and for joint epicentral determination (e.g., Pujol 2000) to simultaneously determine multiple earthquake locations and station corrections related to errors in the velocity model. However, the high-dimensionality of such problems makes direct-search solution difficult and computationally demanding; at the present time these problems are usually performed through large scale, linearized procedures. For these reasons, we mainly consider here absolute location of individual events.

In this article we describe the earthquake location problem and direct-search methods used to perform this location, and we present a number of examples of direct-search location. We do not compare different direct-search location methods or compare direct-search to linearized algorithms, but instead focus on illustrating important features and complexity in earthquake location results. For this reason we emphasize direct, global-search, probabilistic location, which produces general and complete solutions that best illuminate these features and complexity.

III.   The Earthquake Location Problem

An inherently nonlinear problem

In a homogeneous medium with wave speed v and *slowness* defined to be $u = 1/v$, the arrival time, t_{obs}, at an observation point x_{obs}, y_{obs}, z_{obs} of a signal emitted at origin time t_0 from a source location at x_0, y_0, z_0 is,

$$t_{obs} = t_0 + u\left[\left(x_{obs} - x_0\right)^2 + \left(y_{obs} - y_0\right)^2 + \left(z_{obs} - z_0\right)^2\right]^{1/2}, \qquad (1)$$

This expression shows that a change in the spatial position of the source introduces a nonlinear change in t_{obs}, even in the simplest possible medium. When the speed v and hence slowness u are inhomogeneous in space, the arrival time at the observation point becomes,

$$t_{obs} = t_0 + \int_{\mathbf{r}_0(s)} u(\mathbf{r}_0)\, ds, \qquad (2)$$

where $r_0(s)$ denotes a point at distance s along ray path $\mathbf{r}_0$ between source and receiver locations. Equation (1) is a special case of (2) that has straight source-receiver ray paths. Equation (2) is nonlinear since a change in the source location changes the ray path over which the integral is calculated. Thus, earthquake location, which maps arrival times into spatial location and origin time, is inherently a nonlinear problem.

The observed data

Data used to constrain earthquake locations are usually derived from seismograms recorded at seismic stations distributed around the earthquake source area, usually at or near the surface of the Earth. The derived data for earthquake location include arrival times, polarization angles, or array slownesses and azimuths. For earthquake location there are three important aspects of this data determination: 1) choosing locations for the stations (before data have been collected), 2) deriving data and associated uncertainties from the seismograms, and 3) association of the derived data into subsets of data corresponding to unique events.

The first important aspect of data determination is choosing station locations with the goal of constraining as tightly as possible event locations for a given source area; this is classified as a problem of "experimental design" in the field of statistics. The design problem must be resolved prior to data collection and so is posed in terms of *expected* data, and *expected* location results. We describe experimental design techniques in more detail later, after introducing and discussing the location solution on which such designs depend.

Once stations are installed and have recorded seismograms from earthquakes of interest, a data set must be extracted that is sensitive to the event source location, and which we can associate with some physics (e.g., *P* or *S* waves) and paths of wave propagation. Most commonly for earthquake location the data set will be phase arrival times and associated uncertainties picked manually or automatically from seismograms (Figure 1). It is often easy to detect and pick arrivals manually since the human eye can identify a change in amplitude or frequency in the signal even in the presence of significant noise. The picking of the *S* phase is sometimes more difficult because it arrives in the *P* coda and can be preceded by converted phases; this is a common problem with recordings at local (e.g., up to about 100 km) and near-regional (e.g., up to about 300 km) distances, especially if horizontal component seismograms are not available. The automatic detection, identification and picking of *P* and *S* arrivals is much more difficult, especially in the presence of high noise levels. However, automatic detection and picking is faster and, for the case of initial *P* phases or other phases with characteristic forms, can produce a more consistent data set than manual processing. Automatic arrival detection relies on identifying temporal variations in energy, frequency content, polarization or other characteristics of the signal which are anomalous relative to their background or noise level. Often the detection and picking algorithms are applied to filtered and processed time-series in order either to reduce noise, or to augment the signal in pre-set or dynamically-determined frequency bands or polarization directions. See Gentili and Michelini (2006) for an approach that exploits neural networks for phase identification and picking, and Withers et al. (1998) for a review and systematic comparison of several approaches to

automatic detection and picking.

The data used for earthquake location (e.g., arrival times) must have associated uncertainty estimates otherwise the location uncertainty and a probabilistic solution (i.e., location *pdf*) can not be calculated. Most generally, a vector **d** describes the data takes values from a data space ***D***, and *p*(**d**) denotes the *pdf* representing uncertainty in **d**. The uncertainty in arrival time data should include not only an estimate of the uncertainty in the picked phase arrival time, but also uncertainty in which phase (e.g., *P* or *S*) is associated with the pick. If there are multiple expected phase arrivals close to the picked arrival time of a phase, then ideally these should all be taken as candidate phase types for the arrival. Also, the pick uncertainty of each phase may be best described by a *pdf* that is asymmetric in time, since usually a latest-possible time for a pick is much easier to define than the earliest time (Figure 1). True data uncertainty *pdf*'s are therefore generally multi-modal, and can be quite complex to calculate and parameterize. In practice, an enumerated quality indication or, at best, a simple normal distribution (Gaussian uncertainty) is used to describe the picking error, and the phase association is usually fixed (*e.g.* to *P* or *S*) so corresponding uncertainties are ignored. In many cases these simplified data uncertainty estimates will lead to bias or increased error in the resulting event locations.

The third important aspect of data determination is the association of the derived data into sets of data for unique events. For example, this association may entail the assignment of each arrival time obtained within a specified time window to a unique event, forming the minimum possible number of events and corresponding arrival time sets required to explain observed data. This association procedure can be very difficult, especially with automatic systems and when there are signals from multiple seismic events that are close or overlapping in time (e.g., Johnson et al., 1994), and we do not address this issue further here. In the following, except for an examination of outlier data, we implicitly assume that location is performed with a data set that is already associated to a unique event.

The velocity or slowness model

The velocity or slowness model specifies seismic wave-speeds in the region of the Earth containing the sources, the receivers and the ray paths between the sources and receivers. Equation (2) is nonlinear with respect to source location, but also with respect to slowness since a change in the slowness distribution of the medium changes the ray path. The velocity structure is sometimes estimated through coupled, simultaneous inversions for velocity structure and event locations (commonly called seismic tomography), but these are very large inverse problems solved mainly with linearized methods. Usually for earthquake location the velocity model is taken as known and fixed.

Often, for computational convenience or due to lack of information, the velocity model is parameterised with velocity varying only with depth. This is commonly called a laterally homogeneous or 1-dimensional (1D) model. Such a model may consist of one or more layers of constant or vertical-gradient wave-speeds. For work at a local or near-regional scale the layers may be horizontal and flat; for larger, regional or global scale problems the layers should be spherically symmetric shells to represent the curvature of the Earth. When more information on the velocity structure is available, a 3D model may be used in order to increase the accuracy of the ray paths and travel times, and hence of the locations, relative to a 1D model. All models, whether 1D or 3D, are described by a limited number of parameters and include some form of spatial averaging or interpolation with respect to the true Earth. Although 3D models can potentially represent velocity variations in the Earth more accurately than 1D models, in practice the velocities in 3D models can locally be poorly constrained and have large errors. It is therefore often important to consider several different possible 1D and 3D velocity structures in a location study, either to test the sensitivity of the locations to errors in velocity, or to better estimate the travel-time uncertainties and produce a more

meaningful location *pdf*. In principle the use of diverse velocity models poses no difficulties with direct-search location methods.

The travel-time calculation

The theoretical seismic wave travel-times through a given velocity model between any particular source and receiver locations are required by most location algorithms. The calculation of travel times is commonly referred to as forward modelling, because inverse theory need not be invoked. There are three basic classes of methods to calculate the travel times: full-waveform methods, ray methods, and Huygens wavefront or eikonal methods.

Full-waveform methods (e.g., Aki and Richards, 1980) produce complete synthetic seismograms from which predicted travel times can be extracted. These methods include frequency–wavenumber or modal-summation techniques which are valid for a broad range of frequencies and can produce exact waveforms, but which are only applicable for relatively simple velocity structures. Numerical techniques such as finite elements and finite differences can accurately model full wave phenomena in complicated structures, but these methods typically require large computing resources and computing time. Currently, full-waveform methods are rarely used to determine predicted travel times for earthquake location because these times can be obtained directly and more efficiently with ray and eikonal methods.

Ray methods (e.g., Aki and Richards, 1980; Červený, 2001; Thurber and Kissling, 2000) provide travel times and the path, or ray, travelled by high-frequency waves, and can be applied to complicated and 3D velocity structures. With simple model parameterizations such as flat layers with constant or gradient velocity, ray paths and travel times can be determined very rapidly with analytical or semi-numerical algorithms. For these and more complicated models, shooting, or ray tracing techniques generate rays though iterative solution of a set of ray-tracing equations starting in a specified direction at the source or receiver location. The ray that passes through a specified end point is found by a search over the direction at the starting point; this search can be time consuming or unstable. In addition, shooting methods do not produce diffracted arrivals (e.g., "head waves" from the Mohorovičić discontinuity) which are often the first arriving signal at near-regional distances and thus critical for earthquake location. Two-point, ray bending and perturbation techniques rely on Fermat's principle of least time: an initial guess at the ray between two points is perturbed repeatedly to attain a minimum travel time and corresponding ray between the points. These techniques perform best with smooth models, but do produce diffracted arrivals. In general, except for analytical or semi-numerical algorithms in simple models, ray methods are too computationally expensive for direct-search location, which usually requires evaluation of travel times between a very large number of source and receiver positions. However, some ray bending methods (*e.g.*, Um and Thurber, 1987; Moser et al., 1992b) are efficient enough to be used in direct-search location when a relatively small number of source and receiver positions position need to be examined.

Wavefront, eikonal and graph-based methods (Thurber and Kissling, 2000) provide travel-times of the first arriving, high frequency waves including diffracted arrivals, and are efficient and applicable with complicated, 3D velocity structures. In effect, these methods propagate wavefronts through a velocity model with repeated application of Huygen's principle, by considering a large number of virtual sources (*Huygens sources*) along each wavefront. At time t these sources emit circular wavelets which expand for a small time Δt through the (constant) local, medium velocity. The locus of the first arriving circular wavelets defines the new wavefront location at time $t+\Delta t$. The synthetic travel time of the first-arriving energy at the receiver is the time at which a wavefront first touches the receiver. In practice, this problem is solved on a computer either by replicating this "wavefront marching" process

(e.g., Sethian, 1999; Rawlinson and Sambridge, 2004a), or by finding a numerical solution to the eikonal equation (e.g., Vidale, 1988; Podvin and Lecomte, 1991), or by graphical analysis (e.g., Moser et al., 1992a). Though wavefront, eikonal and graph-based methods produce directly only the travel time of the first-arriving signal, information about the path travelled by the signal can be derived numerically from the travel-time field or from ray-tracing, and travel-times of secondary arrivals can be obtained through multi-stage calculations (e.g., Podvin and Lecomte, 1991; Rawlinson and Sambridge, 2004b).

Wavefront, eikonal and graph-based methods can efficiently generate the travel-times from one point in a gridded velocity model to all other points in the model. This makes these methods particularly useful for direct-search location, which may test a large number of possible source positions widely distributed in space. For this purpose, the travel times from each seismic station to all points in the model can be pre-calculated and stored in computer disk files or in memory; obtaining the travel time from a station to any other point then reduces to a simple lookup (*e.g.*, Moser et al., 1992a; Lomax et al., 2001).

A complete solution - probabilistic location

Consider a vector $\mathbf{d}_{obs}$ of observed data (*e.g.*, arrival times) that takes values in a data space *D,* and let $p(\mathbf{d})$ be the *pdf* over *D* describing the data uncertainty in $\mathbf{d}_{obs}$ due to measurement and processing uncertainties. Similarly, let $\mathbf{m}$ denote the vector of source location parameters (spatial coordinates and origin time) which take values from parameter space *M*. Let $p(\mathbf{m})$ be the prior *pdf* representing all information available about the location before (prior to) using the data $\mathbf{d}_{obs}$; $p(\mathbf{m})$ might include knowledge of the known, active fault zones in the area, or might specify the bounds of a region within which we know the event occurred from damage reports, or of a region containing the network of stations that recorded the event. Also consider the forward problem (*e.g.*, travel time calculation) relating $\mathbf{m}$ to a vector of predicted data (*e.g.*, arrival times), $\mathbf{d}_{calc}$. In general the forward problem may also be uncertain, for example due to uncertainties in velocity structure, so we use $F(\mathbf{d},\mathbf{m})$ to denote the *pdf* of the relationship between $\mathbf{d}_{calc}$ and $\mathbf{m}$ as constrained by the forward problem.

As an example of *F*, it is commonly assumed that for each particular $\mathbf{m}$, the corresponding predicted data $\mathbf{d}_{calc}$ are given by a function $\mathbf{f}(\mathbf{m})$ with negligible errors. Then the conditional *pdf* $F(\mathbf{d} \mid \mathbf{m})$ (the probability distribution of $\mathbf{d}$ when $\mathbf{m}$ is fixed at a particular value) is described by $F(\mathbf{d}|\mathbf{m}) = \delta[\mathbf{d} - \mathbf{f}(\mathbf{m})]$ where δ is the Dirac delta-function. Also, the forward problem is often assumed to place minimum possible constraint on parameters $\mathbf{m}$; the *pdf* describing this state of information about $\mathbf{m}$ is called the homogeneous distribution, represented by $\mu(\mathbf{m})$. No *pdf* exists that describes zero information, but *some* information about $\mathbf{m}$ always exists in practice (the positivity of parameter values, for example); $\mu(\mathbf{m})$ describes that minimum state of information. In that case the forward problem is given by (Tarantola and Valette, 1982; Tarantola 2005),

$$F(\mathbf{d}, \mathbf{m}) = \delta[\mathbf{d} - \mathbf{f}(\mathbf{m})] \, \mu(\mathbf{m}). \tag{3}$$

A solution to the earthquake location problem is found by combining the information in the observed data, $p(\mathbf{d})$, the prior *pdf,* $p(\mathbf{m})$, and the ability of the forward problem to predict the observed data, $F(\mathbf{d},\mathbf{m})$ (Tarantola and Valette, 1982; Tarantola, 2005). This is achieved in a probabilistic framework by constructing a *pdf Q* describing the state of posterior (post-experimental) information by:

$$Q(\mathbf{d}, \mathbf{m}) = k \frac{p(\mathbf{d}) F(\mathbf{d}, \mathbf{m}) p(\mathbf{m})}{\mu(\mathbf{d}, \mathbf{m})}, \tag{4}$$

where the constant k normalizes Q to unit integral over $\mathbf{D} \times \mathbf{M}$ and $\mu(\mathbf{d},\mathbf{m})$ is the homogeneous distribution over data $\mathbf{d}$ and parameters $\mathbf{m}$. Equation (4) contains all information (from the prior, data and physics) that could have a bearing on location $\mathbf{m}$, and defines a joint *pdf* between parameters $\mathbf{m}$ and data $\mathbf{d}$. The final, posterior state of information about location parameters $\mathbf{m}$ is given by integrating over the data $\mathbf{d}$ to obtain the marginal posterior *pdf*,

$$Q(\mathbf{m}) = k \; p(\mathbf{m}) \int_{\mathbf{D}} \frac{p(\mathbf{d})F(\mathbf{d},\mathbf{m})}{\mu(\mathbf{d},\mathbf{m})} \, d\mathbf{d} . \tag{5}$$

Equation (5) is the general, probabilistic solution to the inverse problem of event location from the available data since it describes the uncertainty in event location $\mathbf{m}$ given all available information. It is usual to call the integral in (5) the *likelihood* function $L(\mathbf{m})$, which gives a (non-normalized) measure of how good any model $\mathbf{m}$ is in explaining the observed data $p(\mathbf{d})$.

As mentioned earlier it is often the case that $p(\mathbf{d})$ for the observed data is approximated by a Gaussian distribution, described by mean $\mathbf{d}_0$ and covariance matrix $\mathbf{C}_d$. Assuming that the uncertainties in the forward problem F relating $\mathbf{d}$ and $\mathbf{m}$ are negligible results in the form of F in equation (3). It is also usually assumed that $\mathbf{d}$ and $\mathbf{m}$ are independent and hence that $\mu(\mathbf{d}, \mathbf{m})$ can be written $\mu(\mathbf{d}) \, \mu(\mathbf{m})$; $\mu(\mathbf{d})$ is usually taken to be constant. With these simplifications, used by many current direct-search location procedures, the (non-normalised) likelihood function is given by,

$$L(\mathbf{m}) = \exp\left\{ -\frac{1}{2}[\mathbf{d}_0 - \mathbf{f}(\mathbf{m})]^{\mathrm{T}} \mathbf{C}_d^{-1} [\mathbf{d}_0 - \mathbf{f}(\mathbf{m})] \right\} . \tag{6}$$

With the above simplifications a maximum likelihood origin time, t_0, can be determined analytically from weighted means of the observed arrival times and the predicted travel times (e.g., Tarantola and Valette, 1982), and if the observed and predicted times are uncorrelated we arrive at a likelihood function,

$$L(\mathbf{x}) = \exp\left\{ -\frac{1}{2} \sum_i \frac{\left[T_i^o - T_i^c(\mathbf{x}) \right]^2}{\sigma_i^2} \right\} , \tag{7}$$

where $\mathbf{x}$ is the spatial part of $\mathbf{m}$, T_i^o are observed travel times, T_i^c are the calculated travel times for observation i (i.e., T_i^c represents the travel time, rather than arrival time, part of $\mathbf{f}(\mathbf{m})$), and σ_i summarizes the associated standard deviation of uncertainty in T_i^o and T_i^c.

Though not normalized, $L(\mathbf{x})$ is sufficient to provide the *relative* probability of any location $\mathbf{m}$ being the best estimate of the event location given the available data measurements. Since in practice integrating over all of $\mathbf{D} \times \mathbf{M}$ to find normalizing constant k in equation (5) is often computationally intractable, the product of the prior, spatial location information $p(\mathbf{x})$ (*i.e.*, the spatial part of $p(\mathbf{m})$) and the non-normalized likelihood $L(\mathbf{x})$ is usually taken as the objective function for inversion and searching in direct-search location algorithms. If $L(\mathbf{x})$ is determined throughout the prior *pdf* $p(\mathbf{x})$ through a global-search, then equation (5) can be normalized approximately after location. In the following text and examples, we refer to such an approximately normalized function, $p(\mathbf{x})L(\mathbf{x})$, as a location *pdf*.

The likelihood function in equation (5) is entirely defined by the probabilistic error processes involved. However, often it is desirable to change the approximations employed in deriving equations (6) and (7) from equation (5), in order to remove biases or instability in the solution. The approximation in

equation (6) uses the exponential of an L2-norm misfit function (the term in braces {} in equation 6 or 7) to represent the *pdf* of the data error variation, but because data used for location often contain outliers it is often considered that an L1 norm or other L*p* norm (*p* < 2.0) is more appropriate (e.g., Shearer, 1997), where $Lp\text{-norm}|\mathbf{x}| = \sqrt[1/p]{\sum |x_i|^p}$. Earthquake location problems formulated with an L*p* norm (or indeed other kinds of likelihood functions – see equation (8) below), can be solved relatively easily with direct-search methods, which, unlike linearized methods, do not require determination of partial derivatives of the likelihood or objective function with respect to event location.

An alternative to L*p*-likelihood functions that is very robust in the presence of outliers is given by the equal differential-time (EDT) formulation (Zhou, 1994; Font et al., 2004; Lomax, 2005). For the EDT case, the location likelihood is given by,

$$L(\mathbf{x}) = \left[\sum_{a,b} \frac{1}{\sqrt{\sigma_a^2 + \sigma_b^2}} \exp\left(-\frac{\{[T_a^o - T_b^o] - [TT_a^c(\mathbf{x}) - TT_b^c(\mathbf{x})]\}^2}{\sigma_a^2 + \sigma_b^2} \right) \right]^N , \qquad (8)$$

where **x** is the spatial part of **m**, T_a^o and T_b^o are the observed arrival times and TT_a^c and TT_b^c are the calculated travel times for two observations *a* and *b*; the sum is taken over all pairs of observations, and *N* is the total number of observations. Standard deviations σ_a and σ_b summarize the assigned uncertainties on the observed arrival times and calculated travel times, where it is assumed that the observed and the calculated times are uncorrelated.

In Equation (8), the first and second terms in brackets in the exponent are, respectively, the differences between the observed arrival times and the differences between the calculated travel times. The exponent is the difference between these two terms, and thus the exponential has a maximum value of 1 which occurs at points **x** where the two differences are equal (hence, the name "equal differential time"). Such points **x** best satisfy the two observations *a* and *b* together, and, in general, the set of **x** where the exponential is nonzero forms a "fat," curved surface in 3D space. Because the summation over observations is outside the exponential, the EDT location *pdf* has its largest values for those points **x** where the *most* pairs of observations are satisfied and thus is far less sensitive to outlier data than L*p* norms which seek to best satisfy *all* of the observations simultaneously. Note that the EDT likelihood function *L*(**x**) does not require calculation of an origin time t_0; this reduces the hypocenter search to a purely 3-parameter problem and contributes to the robustness of the EDT method. Nevertheless, a compatible estimate of t_0 can be calculated for any hypocenter point **x**.

Ultimately, the full solution to the probabilistic location problem is a posterior *pdf* which includes as comprehensive as possible uncertainty information over parameters **m**. This may include multiple "locally-optimal" solutions, e.g., *Q*(**m**) or *p*(**x**)*L*(**x**) may have multiple maxima, and may have a highly irregular form. Some studies of seismicity and seismotectonics make explicit use of a probabilistic representation of seismic event locations (e.g., Presti et al., 2004; Husen and Smith, 2004; Lomax, 2005).

Experimental design methods – choosing receiver locations

As noted earlier, it is important to position stations so as to constrain as tightly as possible the event locations for a given source area. The location inverse problem solution in equations (5), (7) or (8) is constrained by prior information on location *p*(**m**), by observed data *p*(**d**), and by forward-problem physics relating **d** and **m**. One way to significantly influence the form of this inverse problem, and hence uncertainty in its solution, is to change the data we record. Thus, we alter both *p*(**d**) and the

forward-problem physics, $F(\mathbf{d}, \mathbf{m})$.

For seismic location problems we may change the data by employing experimental design methods to choose or change the locations of seismic receivers. The goal of the design procedure is to place receivers such that the location information described by solution $Q(\mathbf{m})$ is expected to be maximised. This is a "macro-optimisation" problem where, prior to the occurrence of an earthquake, we optimise the design of the inverse problem that we expect to solve after an earthquake has occurred.

The design is varied such that it maximises an objective function. This is usually taken to be the expected value of some approximation to the unique measure of information that was discovered by Shannon (1948),

$$J(\mathbf{R}) = E_{\mathbf{m}_t} \left\{ I\left[Q(\mathbf{m}); \mathbf{R}, \mathbf{m}_t \right] \right\} \tag{9}$$

where $\mathbf{R}$ is a vector describing the design (e.g., receiver locations), $I[Q(\mathbf{m}); \mathbf{R}, \mathbf{m}_t]$ is the information contained in the resulting posterior *pdf* $Q(\mathbf{m})$ for design $\mathbf{R}$ when the true parameters (e.g., event location) is $\mathbf{m}_t$, and the statistical expectation $E_{\mathbf{m}_t}$ is taken over all possible $\mathbf{m}_t$ which (according to our prior knowledge) are expected to be distributed according to the prior distribution $p(\mathbf{m})$. $J(\mathbf{R})$ should be maximised.

Within the expectation in equation (9), the design criterion $J(\mathbf{R})$ takes account of all possible potential true event locations $\mathbf{m}_t$, their prior probability of occurrence $p(\mathbf{m})$, and the corresponding data (including their uncertainties) that are expected to be recorded for each location (the latter are included within $Q(\mathbf{m})$). To calculate the expectation usually requires integration over a far greater proportion of the model and data spaces, *M* and *D* respectively, than need be considered when solving the inverse problem after a particular event has occurred (since then $p(\mathbf{d})$ and hence $Q(\mathbf{m})$ are fixed, and $p(\mathbf{m})$ is more tightly constrained). Consequently, experimental design is generally far more computationally costly than solving any particular inverse problem post-event.

For this reason, design methods invoking linearized approximations to the model-data relationship $F(\mathbf{m}, \mathbf{d})$ (e.g., equation 10 below) have been employed by necessity in the past (Steinberg et al., 1995; Rabinowitz and Steinberg, 2000; Curtis 2004a; Curtis et al., 2004), or indeed non-probabilistic methods have been employed (e.g., Maurer and Boerner 1998; Curtis, 1999a,b; Stummer et al., 2004). Truly non-linearized design methods have been developed for location problems only relatively recently (van den Berg et al., 2003; Curtis 2004b; Winterfors and Curtis, 2007). Historically, however, station network geometry has been defined more by heuristics (rules of thumb) and geographical, logistical and financial constraints, with design theory only recently being deployed.

IV. Location methods

Once data have been recorded and prior *pdf*'s defined, a solution such as that of equations (5), (7) or (8) must be evaluated throughout the prior *pdf*, $p(\mathbf{x})$, to identify one or more locally-optimal" solutions, or, preferably, to obtain a full probabilistic location *pdf*. This evaluation generally requires direct-search optimisation and search techniques, which we discuss below. We first digress and summarize linearized location procedures, which typically determine a single optimal hypocenter along with a simplified and approximate representation of the location *pdf* (*e.g.*, a confidence ellipsoidal centred on the estimated hypocenter and origin time).

Linearized location methods

With linearized methods the arrival time expression (2), which is nonlinear with respect to the spatial

location $\mathbf{m}=(x, y, z)$, is approximated by a Taylor series expansion around some prior estimate $\mathbf{m}_0=(x_0, y_0, z_0)$ of the spatial location:

$$f(\mathbf{m})= f(\mathbf{m}_0)+(\mathbf{m}-\mathbf{m}_0)f'(\mathbf{m}_0)+\frac{(\mathbf{m}-\mathbf{m}_0)^2}{2}f''(\mathbf{m}_0)+ O[(\mathbf{m}-\mathbf{m}_0)^3] \qquad (10)$$

where $f(\mathbf{m})$ is the forward problem that calculates an arrival time d_{calc} given a location $\mathbf{m}$ (e.g., $f(\mathbf{m})$ might represent the right hand side of equation (2) directly). A linear vector-matrix inverse problem is obtained if we approximate the forward problem for all $\mathbf{d}_{calc}$ by using only the first two terms of the Taylor series. The resulting vector-matrix equation may be solved using linear algebraic methods. This process is called *linearized inversion*.

Usually, this linearized inversion is iterated: the prior estimate $\mathbf{m}_0$ is set equal to the newly-found, best-fit location, the problem is re-linearized around this new estimate using equation (10), and the new linear problem solved again. This method may be repeated (iterated) many times, as needed to attain some convergence criteria.

Linearized methods produce a single, best-fit (e.g., maximum likelihood) hypocenter and origin time location, and associated, linearly-estimated uncertainties, such as a multi-dimensional, normal-distribution centred on the best-fit hypocenter and origin time. However, this linearized solution is often a poor representation of the complete solution *pdf* (Figure 2 and see examples), and it may be unstable when the *pdf* is irregular or has multiple peaks due to insufficient or outlier data, velocity model complexities, and other causes (*e.g.*, Buland, 1976; Lomax et al., 2000).

Direct-search location methods

The earliest, formal earthquake locations from phase arrival time observations used nonlinearized procedures. Milne (1886) describes and applies several graphical and algebraic methods to determine earthquake locations. These include a perpendicular bisector method for the case of 3 or more simultaneous arrival time observations (related to the modern arrival order or bisector method, described below), a method of hyperbolae based on the differences in arrival times at pairs of stations (related to the modern EDT method, described below) and a method using the differences in arrival times of different wave types at individual stations. The latter is a generalization of the method of circles using *S-P* times, in which the distance from a station to the source is, for given *P* and *S* velocity models, a function of the difference of the *S* and *P* arrival times; an epicentre can be constrained with such *S-P* based distances from 3 stations. Reid (1910) determined a hypocenter location for the great 1906 California earthquake through a coarse, systematic grid search over velocity, position along the causative fault and depth, solving for the origin time and wave velocity by least-squares at each grid point.

The arrival order or bisector method (Anderson, 1981; Nicholson et al., 2004a) is a nonlinear, geometrical approach that uses the constraint that if a phase arrival is earlier at station A than at station B, then the event is closer to A than to B (assuming the velocity model is such that arrival order implies distance order). Applying this constraint to all pairs of stations defines a convex region containing the event location. This method is useful for obtaining some constraint on the location of events far outside of an observing station network, and for rapidly and robustly obtaining starting locations for linearized methods.

Most other modern, direct-search earthquake location methods (excluding graphical methods that are now mainly used for illustrative and educational purposes) are based on deterministic or stochastic searches which may be exhaustive or directed and evolutionary. These searches are used to explore or map likelihood functions such as those given in equations (5), (7) or (8). When these searches gather

and retain information globally, throughout the prior *pdf* $p(\mathbf{x})$, they can produce a complete, probabilistic location *pdf*. Otherwise, searches may determine a global or local maximum of the location *pdf*, or may explore the neighbourhood around these optimal points to locally estimate the *pdf* and obtain uncertainty information.

Regular, deterministic search

Regular and deterministic searches, such as grid-searches, nested grid-searches and stochastic, "crude" Monte-Carlo searches (e.g., Hammersley and Handscomb, 1967; Sambridge and Mosegaard, 2002) use global and well-distributed sampling of the model space and thus can estimate the complete location *pdf*. All of these approaches are computationally demanding for problems with many unknown parameters, large parameter spaces, or time consuming forward calculations, because the number of models that must be tested can be very large. These methods have been successfully applied to the determination of optimal hypocenters (*i.e.*, Sambridge and Kennett, 1986; Kennett, 1992; Shearer, 1997; Dreger, et al. 1998), and to probabilistic location (*i.e.*, Moser et al., 1992a; Wittlinger et al., 1993; Calvert et al., 1997; Lomax et al., 2000), but their inefficiency may impose unacceptable limitations on the number of events that can be considered, or on the size of the search volume.

Directed search

Directed, stochastic search techniques include evolutionary, adaptive global search methods such as the genetic algorithm (Goldberg, 1989; Sambridge and Drijkoningen, 1992) and simulated annealing (Kirkpatrick et al., 1983; Rothman, 1985; Tarantola, 1987). The simplex method is a directed, deterministic search technique that is nonlinearized and can be used for earthquake location (*e.g.*, Rabinowitz, 2000). Most of these methods were developed for optimization or the identification of some very good solutions, which is equivalent to identifying a global or local maximum of the location *pdf*. In general, these methods do not explore the prior *pdf* $p(\mathbf{x})$ in a manner that can produce complete, probabilistic solutions to inverse problems. For example, the genetic algorithm performs global searching and may be one of the most efficient stochastic methods for optimization, but it does not use well distributed sampling (the sampling tends to converge rapidly to the region of a locally optimum solution). Similarly, in the simulated annealing, random-walk method the interaction of its variable "temperature" parameter and step size with the local structure of the misfit function can lead to convergence and stalling near a locally optimum solution, and a sample distribution that is neither well nor globally distributed. Both the genetic algorithm and simulated annealing can be tuned to sample more broadly and in the limit become crude Monte Carlo searches, but this removes the main advantage of these methods – that of rapid stochastic optimization.

Though not directly applicable to complete, probabilistic location, directed search algorithms are useful for direct-search, earthquake hypocentre estimation because of their efficiency (*e.g.*, Sambridge and Kennett, 1986; Sambridge and Gallagher, 1993; Billings, 1994; Rabinowitz, 2000).

Importance sampling

The efficiency of a Monte Carlo algorithm used to estimate properties of a target (misfit or likelihood) function can be increased by choosing a sampling density which follows the target function as closely as possible (Hammersley and Handscomb, 1967; Lepage, 1978; Press et al., 1992). Techniques that follow this rule are referred to as importance sampling methods, and were originally developed in physics for fast and accurate numerical integration of multi-dimensional functions. The target function is unknown, however, and consequently the optimum importance sampling distribution cannot be determined a priori. Instead, improved efficiency is attained by adjusting (or adapting or evolving) the

sampling by using information gained from previous samples so that the sampling density tends towards the target function as the search progresses (Lepage, 1978; Press et al., 1992; Mosegaard and Tarantola, 1995; Sen and Stoffa, 1995). For example, importance sampling to determine an earthquake location *pdf* or likelihood function (e.g., equation (5), (7) or (8)), can be obtained by beginning with a sampling that follows the prior *pdf*, $p(\mathbf{m})$, and then adjusting the sampling as the search progresses so that the sampling density approaches the location *pdf*.

Importance sampling techniques that can be used to find complete, probabilistic solutions to inverse problem include the VEGAS algorithm (Lepage, 1978), the Metropolis algorithm (Mosegaard and Tarantola, 1995), the neighbourhood algorithm (Sambridge, 1998) and, for three-dimensional problems, oct-tree (Lomax and Curtis, 2001). Other importance sampling methods are discussed in Hammersley and Handscomb (1967) and in Press et al (1992) in the context of numerical integration.

The VEGAS algorithm (Lepage, 1978; Press et al, 1992) performs importance sampling by accumulating appropriate sampling distributions independently for each parameter as the sampling proceeds. This method can give very good estimates of an individual or a joint marginal *pdf*, but it looses efficiency if the target function includes strong correlation between parameters or if it is independent of some parameters (Press et al, 1992). In addition, the VEGAS algorithm may be difficult or impossible to implement with prior information, such as smoothness constraints, that introduces correlation between parameters. Consequently, this algorithm may not be appropriate for some geophysical problems, including earthquake location, when the location parameters are often correlated or poorly resolved.

The Metropolis or Metropolis-Hastings algorithm (e.g., Mosegaard and Tarantola, 1995) is similar to simulated annealing but with a constant temperature parameter. The Metropolis algorithm performs a random walk in the model space, testing at each step nearby trial samples which are accepted or rejected after evaluation of the forward problem according to a likelihood $L(\mathbf{m})$. Mosegaard and Tarantola show that this algorithm samples from the posterior *pdf* of the problem and is therefore an importance sampling method. They show that, in the limit of a very large number of trials, it will not become permanently "trapped" near local maxima and consequently will produce global sampling. Also, because it is a random walk technique, the Metropolis algorithm can perform well even if the volume of the significant regions of the posterior *pdf* is small relative to the volume of the prior *pdf*. However in practical application this algorithm can become trapped in strong local maxima of the posterior *pdf* if this function is complicated. The Metropolis algorithm has been applied to earthquake location in 3D structures by Lomax et al. (2000) and Lomax et al. (2001).

Another recently developed importance sampling technique used in geophysics is the neighbourhood algorithm (Sambridge, 1998, 1999a, 1999b), applicable to high dimensional model spaces. Given an existing set of samples of the objective function, the neighbourhood algorithm forms a conditional *pdf* using an approximate Voronoi cell partition of the space around each sample. The algorithm generates new samples through a uniform random walk within the Voronoi cells of the best fitting models determined so far. This algorithm is applied to the 4D hypocentre location problem in Sambridge (2003) and in Kennett (2006).

The oct-tree importance-sampling method (Lomax and Curtis, 2001) uses recursive subdivision and sampling of rectangular cells in three-dimensional space to generate a cascade structure of sampled cells, such that the spatial density of sampled cells follows the target *pdf* values. The relative probability that an earthquake location is in any given cell i is approximately,

$$P_i = V_i L(\mathbf{x}_i), \tag{11}$$

where V_i is the cell volume and $\mathbf{x}_i$ is the vector of coordinates of the cell centre. Oct-tree importance-

sampling is used to determine a location *pdf* by first taking a set of samples on a coarse, regular grid of cells throughout the search volume. This is followed by a recursive process which takes the cell *k* that has the highest probability P_k of containing the event location, and subdividing this cell into 8 child cells (hence the name oct-tree), from which 8 new samples of the *pdf* are obtained. These samples are added to a list of all previous samples, from which the highest probability cell is again identified according to equation (11). This recursive process is continued until a predetermined number of samples are obtained, or until another termination criterion is reached.

For most location problems, including those with a complicated location *pdf,* the oct-tree recursive subdivision procedure converges rapidly and robustly, producing an oct-tree structure of cells specifying location *pdf* values in 3D space. This oct-tree structure will have a larger number of smaller cells in areas of higher probability (lower misfit) relative to areas of lower *pdf* value and thus the oct-tree method produces approximate importance-sampling without the need for complex geometrical constructs such as Voronoi cells. Oct-tree sampling can be used with the L2-norm likelihood function in equation (7) or the EDT likelihood function in equation (8), since both require searching over three-dimensional spatial locations only. Oct-tree sampling has been applied to earthquake location in 3D structures by Husen *et al.* (2003), Husen and Smith (2004), Lomax (2005) and Lomax (2008); we use this sampling method to determine locations in the examples presented below. Though limited to determination of the 3D, spatial location, it is possible that this recursive sampling procedure can be extended to 4D to allow determination of the origin time.

V.   Illustrative Examples

We illustrate the concepts described in the previous sections using an M3.3 earthquake that occurred in the Garfagnana area of Northern Tuscany, Italy, on March 5, 2007 at 20:16 GMT. The earthquake was recorded by stations of the Italian Seismic Network (ISN) at distances from less than 10 km to more than 300 km. We use manually picked *P* and *S* phase arrival times from the INSN bulletin with Gaussian uncertainties (standard deviations from 0.01 to 0.1 s), and a 1-D velocity model similar to the standard model used by INSN for routine earthquake location in Italy. We perform all event locations with the probabilistic location program NonLinLoc (Lomax, et al., 2000; Lomax, et al., 2001; Lomax, 2005; http://www.alomax.net/nlloc; NLL hereafter), using the oct-tree sampling algorithm (section IV) to perform a global-search within a parameter space *M* formed by a rectangular volume 360 km on each side and from the Earth's surface to 35 km depth (except as noted in figure captions).   We use the L2-norm (equation 7) or EDT (equation 8) likelihood functions to obtain location *pdf*'s in 3D space and corresponding maximum likelihood origin times.

In order to describe the location problem and the solution quality for each of the examples presented below we focus on geometrical properties of the location *pdf*, which represents most completely the results of probabilistic, direct, global-search methodologies. We also consider the maximum likelihood hypocenter, defined as the point in space of the maximum value of the location *pdf*, and the corresponding origin time. We examine statistics of the quality of the solutions using the half-lengths of three principal axes of a 68% confidence error ellipsoid approximation to the location *pdf*, l_{ell}, the weighted, root-mean-square of the arrival residual (observed – calculated) times, *rms*, and a relative measure of the volume of the high likelihood region of the location *pdf*, V_{pdf}, given by,

$$V_{pdf} = \int_{\mathbf{M}} \frac{pdf(\mathbf{x})}{pdf^{\max}} dV \,, \tag{12}$$

where $pdf^{\max}$ is the maximum value of the location *pdf* in *M*. We also make use of standard measures of the experimental design quality (i.e, stations coverage) including the *gap* - the largest angle between

the epicentre and two azimuthally adjacent stations used for location, and the distance Δ_0 from the hypocenter to the closest station. These indicators are summarized in Table 1 for the examples presented here.

These examples are meant to show important features and complexity in earthquake location results, not to compare different direct-search location methods or to compare direct-search to linearized algorithms. However, because linearized earthquake location has been and remains an important and widely used tool, we indicate for each example the location results obtained with a linearized algorithm, Hypoellipse (Lahr, 1999). Hypoellipse uses a least-squares, L2-norm and produces a 68% confidence ellipsoid for the hypocenter location. For well constrained locations this ellipsoid should closely match the *pdf* of our probabilistic, L2-norm locations; we plot the Hypoellipse ellipsoid for cases where it differs notably from the probabilistic location, L2-norm *pdf*.

Example 1: An ideal location

To construct an ideal, reference location and synthetic data set for the 2007 Italian earthquake we first locate the event using the earliest 20 observed *P* or *S* arrival times (Fig. 3; Table 1; example 1a). Next, we subtract the arrival residuals for this location from the corresponding times for all observations and relocate the event with the earliest 50 of these "corrected" times (Fig. 3; Table 1; Example 1b). This procedure results in an ideal, synthetic data set and a location problem that are equivalent to the case of no "a posteriori" picking error and no travel-time error (*i.e.*, no velocity model error). For this problem the quality of the solution and the shape of the resulting location *pdf* reflect primarily the station geometry and corresponding ray take-off angles about the source.

The reference location (Fig. 3; Table 1; Example 1b) has *rms* = 0 s, *gap* = 63˚, $\Delta_0 \sim 9$ km, $V_{pdf} \sim 7.0$ km^3 and l_{ell} = 1.05, 1.32 and 2.05 km. The *rms* is necessarily zero because we used residuals as time corrections, while the other indicators and the near-ellipsoidal form of the location *pdf* show a well constrained location. The location is well constrained by the data because stations are available at a wide range of distances and azimuths. In particular, the presence of a station nearly above the event, and of both *P* and *S*-wave arrival times for the closer stations, give good depth constraint.

Examples 2-5: Station distribution

In the next examples we show locations for three cases with poor station distribution about the source: 1) few available stations; 2) stations all to one side of the event; and 3) no data for stations near or above the source, and we illustrate the application of experimental design techniques to improve the station distribution.

Example 2: Few available stations

We first examine relocations of the 2007 Italian earthquake obtained with different numbers of *P* and *S* arrival times selected from the ideal, synthetic data set (Fig. 4; Table 1; Example 2a-d). With only two stations and 2 arrivals (2 *P* phases) the location *pdf* is a fat, near-vertical, planar surface with an elongated, boomerang shape trending perpendicular to the line connecting the two receivers (Fig. 4a). With the addition of *S* arrivals from the same stations (4 arrivals – 2 *P* and 2 *S* phases) the location *pdf* is greatly reduced in volume, and has the form of an annulus oriented roughly perpendicular to the line connecting the two receivers (Fig. 4b). The annular form of this *pdf* results from the intersection of the boomerang shape *pdf* produced by the 2 *P* phases (Fig 4a.) and two hemispherical *pdf*'s centred on each station. Each of these hemispherical *pdf*'s would be produced by location using only the *P* and the *S* reading from either station; this is the probabilistic analogue to the method of circles using *S-P* times.

With three stations (3 arrivals – 3P phases) the location *pdf* forms one mass and its volume is further reduced. This location *pdf* retains an irregular, curved shape resulting from poor constraint of one spatial dimension that trades off with origin time (Fig. 4c). For all of these locations the problem is effectively underdetermined – the data cannot constrain all three hypocentral coordinates and origin time. In these cases a linearized location algorithm may not converge and would be unable to represent properly the effective location uncertainties. As more data are added, the location *pdf* progressively reduces in size and complexity, and with the addition of a station close to and above the source (8 arrivals – 5 *P* and 3 *S* phases), the location *pdf* has a compact, near ellipsoidal form indicating some constraint on all hypocentral coordinates and origin time (Fig. 4d). This location is similar to that obtained with the complete, ideal data set (Fig. 3b), though the location *pdf* remains much larger than that of the ideal case which has arrival times from many more stations.

Example 3: Stations to one side of the event – large gap

Next, we examine the case of earthquakes occurring outside of the recording network with an example using *P* arrival times from stations only to the southeast of the earthquake (Fig. 5; Table 1; Example 3). The location *pdf* is large and elongated in a northwest-southeast direction oriented towards the centroid of the available stations because the lack of stations to the northwest (and use of *P* times only) allows a strong trade-off between potential hypocenter locations along this direction and origin time. In contrast, there is some constraint of the *pdf* to the northeast and southwest due to the aperture of the available stations. The poor station distribution and potential lack of constraint is clearly indicated by the large gap value for this location, *gap* = 251˚. One or more good quality *S* readings can reduce the elongation of the *pdf*.

Example 4: Stations far from the event – vertically elongated pdf

We next show an example where the nearest recording stations are far from the earthquake, relative to its depth, and either *P* arrival times only or both *P* and *S* arrival times are available (Fig. 6; Table 1; Examples 4a-b). With this station geometry the seismic rays leave the source region with approximately the same dip-direction to all stations. Consequently a change in source depth gives about the same change in predicted travel times to all stations. This change in travel time is indistinguishable from a change in origin time (c.f., Eqs. 1 or 2), leading to a strong trade-off between origin time and depth. Consequently the location *pdf* has a vertically elongated shape which, for the case of *P* arrivals only (Fig. 6a), extends throughout the entire search range in depth indicating no depth constraint. For a linearized location algorithm this location problem can be effectively underdetermined, though most linearized algorithms can fix the hypocenter depth artificially in order to obtain a stable epicentral location. The addition of *S* arrival times (Fig. 6b) improves the depth constraint to some extent, although the location *pdf* remains highly elongated in the vertical direction. The lack of close stations and potential lack of constraint is clearly indicated by the large Δ_0 value for this location, $\Delta_0 \approx 106$ km.

This case is common with sparse networks and with shallow sources. Reducing the vertical extent of the *pdf* requires stations at distances of the order of the source depth or less. The addition of one or more good quality *S* readings, especially at the closest stations, would further improve the depth constraint.

Example 5: Stations selection with experimental design

Next, we illustrate the application of experimental design techniques to station selection (Fig. 7; Table 1; Example 5). Considering a case similar to Example 3, which has 6 stations to one side of the event giving poor constraint on the location, we determine an optimal set of 6 stations to best constrain the

location. To do this we apply a linearized design method (Curtis et al., 2004) to select an optimal subset of 6 of the available INSN stations to best constrain an event at the (known) location produced by the ideal, synthetic data (Example 1b).

The design procedure does not simply select the 6 closest receivers to the source (i.e. first 6 available arrival times, Fig. 7a), but instead selects receivers distributed around, and to a large distance away from the source (Fig. 7b). This choice can be understood as balancing the distribution of directions (azimuth and inclination) that the rays leave the source to the selected receivers, a direct result of the use of the linearized approximations to the model-data relationship (equation 10) in the linearized design method (Curtis et al., 2004). This method is based on selecting stations based on the similarity between the rows of the location kernel matrix of the linearized problem; the approach does not differ significantly from that of Uhrhammer (1980) based on the condition number of the same matrix. The improvement in station distribution in azimuth is indicated by the small gap value for this location, *gap* = 89˚. The resulting location *pdf* (Fig. 7b) is compact and symmetric relative to the location *pdf* obtained from the first 6 stations recording the *P* phases (Fig. 7a), and the maximum likelihood hypocenter is close to the ideal location hypocenter.

Example 6: Incorrect picks and phase identification - outlier data

For a given hypocenter location, an outlier arrival time has a residual that is much greater than its nominal error. Data outliers are common with automatic phase arrival picking algorithms, with *S* arrival picks, for small events, distant stations, or other cases where the signal to noise ratio is low, and for early instrumental data where large timing errors are common. In many cases, such as automatic earthquake monitoring and early warning systems, it is important to have robust location procedures that are influenced as little as possible by the presence of outliers. One way to achieve this is to use robust likelihood functions such as EDT (equation 8). In the example below, we compare the performance of EDT and the more commonly used L2-norm likelihood functions.

This example uses only stations near the source, and arrival times from ideal, synthetic data sets for both the L2-norm and the EDT likelihood functions. We add 3 s to the *P* arrival time at two stations to generate outlier data, and examine L2-norm and EDT locations without and with the outlier data (Fig. 8; Table 1; Examples 6a-d). The L2-norm location with the outlier data (Fig. 8b) does not identify and isolate the two outlier *P*-arrivals but instead mixes information from these arrivals with the other data resulting in relatively large, non-zero residuals for all arrivals. This results in a bias of about 10 km in the maximum likelihood hypocentre location relative to the ideal location hypocenter, while the location *pdf* for the L2-norm locations with and without outlier data have about the same size and form, but have little overlap (Figs. 8a and 8b). Thus the L2-norm solution gives no clear indication of the presence of outlier data, or that the solution may be biased. In contrast, the EDT location for the data set containing the outliers (Fig. 8d) correctly identifies the two outlier arrivals (the EDT residuals for these two outlier data are both about 2.9 s) and strongly down-weights them (from 1.2 to 0.17 posterior weight), while producing small residuals (< 0.08 s) for the remaining arrival, as would be the case without outlier data. The maximum likelihood hypocenters for the EDT locations with and without outlier data are almost identical, but the location *pdf*'s are very different (Fig. 8c and d). With outlier data, the *pdf* has an irregular shape and several distinct parts, reflecting the inconsistency of the data set to constrain a unique event location. For the outlier locations, a potential problem with the data set is indicated by the large *rms* values with both L2-norm and EDT, and with EDT alone, by the asymmetry in residuals, the irregular *pdf* shape, and the large V_{pdf} and l_{ell} values.

This result shows that location in the presence of outlier data can be remarkably stable with the EDT likelihood function, which is easy to implement with direct-search location techniques. In contrast, the

same location with the commonly used, L2-norm likelihood function is biased, while presenting few indicators of this bias.

Example 7: Earthquake early-warning scenario

Location for earthquake early-warning must be performed rapidly and in an evolutionary manner starting with the first available phase arrivals. In this example we examine the ability of direct-search location to obtain robust and useful location information using P arrivals from the first stations that record the Northern Italian event (Fig. 9; Table 1; Examples 7a-d).

Within about 6 seconds after the origin time, t_0, three P reading are available. Location with these readings produces an extensive location *pdf* that fills the southwest quadrant of the search region (Fig. 9a); this *pdf* does not provide useful constraint on the location, but is robust in that it includes the true location. Progressive addition of more arrival time data (Fig. 9b and c) reduces the size of the location *pdf*. With 5 arrivals, at about 7 s after t_0 (Fig. 9c), the maximum likelihood location is close to that of the ideal, synthetic location and the location *pdf* is well delimited, although elongated towards the west because no arrivals are yet available from stations in that direction. By 13 s after t_0 (Fig. 9d), 10 P arrivals are available and the location *pdf* is now compact and symmetrical, primarily because a station to the northwest is included. This *pdf* has small enough V_{pdf} and l_{ell} values to provide useful, probabilistic constraint on the location for early-warning purposes at a regional scale, while the maximum likelihood hypocenter is effectively the same as that of the ideal location. In practical application, direct-search location results similar to those illustrated here can be obtained within a delay of less than 1 sec after the readings are available (e.g. Satriano et al., 2007b).

Example 8: Incorrect velocity model

Any velocity model used for earthquake location is an approximation to the true Earth and thus will in general produce erroneous predicted travel times. The magnitude of error in the travel times depends on many factors, but will in general be larger for more distant stations and with increased complexity in the true Earth structure. We examine the effect of an incorrect velocity models by repeating the ideal location (Example 1a and b) with and without the "corrected" times, and using 50 P arrivals (the ideal location was determined using the first 20 P or S arrivals). We examine locations using the L2-norm and EDT likelihood functions (Fig. 10; Table 1; Examples 8a-d).

The locations with time corrections (Fig. 10a and c) simulate the unrealizable case of perfect knowledge of the velocity structure. With both the L2-norm and EDT the location results show zero residuals, compact location *pdf*'s and a maximum likelihood hypocenter that necessarily matches exactly the corresponding ideal location. We note, however, that the L2-norm and EDT "ideal" locations differ slightly because they are derived from noisy, real data, and they use different likelihood functions.

The locations without time corrections (Fig. 10b and d) use the true observed data (i.e., travel times through the true Earth) and thus show the effect of an incorrect velocity model (i.e., the 1-D velocity model used for location). This is shown by the pattern of positive and negative residuals obtained with both the L2-norm and EDT. The L2-norm location without time corrections has a balanced distribution of positive and negative residuals and, relative to the L2-norm location with corrections, a similar size location *pdf* and a biased maximum likelihood hypocentre. In contrast, the EDT location without corrections has more positive than negative residuals and, relative to the EDT location with corrections, a larger location *pdf* and nearly identical, unbiased maximum likelihood hypocentre. For these locations, a potential problem with the velocity model is indicated by the large residuals and *rms* values with both L2-norm and EDT, and, with EDT, by the asymmetry in residuals, the irregular *pdf* shape,

and the large V_{pdf} and l_{ell} values, as with the outlier data example (Example 6).

In effect, locations with an incorrect velocity model and with outlier data are mathematically similar, though in the former case all or most residuals may be large while in the latter case only a few will be large. It is difficult to distinguish between the two cases with the L2-norm because this algorithm seeks to best satisfy *all* of the observations simultaneously (*cf.*, equation (7)) by balancing the distribution of positive and negative residual (*cf.*, Fig. 8b and Fig. 10b). Thus, relative to the residuals corresponding to the correct location, the L2-norm solution damps and hides larger residuals at the expense of increasing small residuals. In contrast, EDT seeks to best satisfy the *most* pairs of observations (*cf.*, equation (8)) and imposes no inherent constraint on the distribution of residuals. Thus with EDT the difference in number, magnitude and distribution of large residuals - few and large for the outlier case, many of similar magnitude and spatially correlated for the incorrect velocity model case – allows one, in principle, to distinguish between the two cases (*cf.*, Fig. 8d and Fig. 10d). In addition, the size and complexity of the location *pdf*'s generally increases more rapidly with EDT than with the L2-norm as the solution quality decreases. Thus, with both the outlier and incorrect velocity model cases, the location results with the EDT likelihood function are more informative than with the L2-norm. However, location with the EDT likelihood function can become unstable (e.g. define only a local maximum of the *pdf*) for cases where the outlier data or velocity model errors lead to extreme complexity in the topology of the EDT location *pdf*.

VI. Future directions

There are various ways that direct, global-search location methodologies may evolve in the future. For example, the stability and completeness of the location and location *pdf* could be improved with the use of more complete data uncertainties, expressed as a *pdf*. These *pdf*'s may typically be irregular and asymmetric, and difficult to determine and parameterize. Currently, enumerated quality indications or, at best, simple normal distributions (describing Gaussian uncertainty) are used to describe the picking error.

Similarly, we have shown that earthquake location depends inherently on the velocity model adopted, but that no realistic uncertainties are associated with this model. Differences between the velocity model and the true Earth can result in complicated differences in ray-paths and travel-times, which will depend strongly on the source and receiver positions. These complications, combined with the lack of knowledge about the true Earth, makes estimating true travel time uncertainties effectively impossible. However, it can be assumed that changes become progressively larger with increasing ray-path length. This effect could be accounted for approximately by travel-time uncertainties that increase with the ray-length or travel time. Instead of using a velocity model to generate travel times, another approach is to derive the required times from tables of empirically determined or corrected travel times (e.g. Myers and Schultz, 2000; Nicholson et al., 2004b). With this approach the travel-time uncertainties are estimated from timing information, with little or no direct use of velocity structures or ray paths.

We have described and illustrated the importance of the source-receiver geometry for locating earthquakes, notably with regards to constraining a compact and symmetric location *pdf*. Thus, improved constraint on event locations can be achieved through prior use of survey design techniques to select station sites. In a related manner, after an event occurs, these techniques could be employed dynamically to weight the available arrival times used for location with respect to the geometry of the available stations around the likely source region.

The demand for rapid, real-time location and earthquake early warning requires improvements in the integration, speed, quality and robustness of the phase arrival picking, phase association and event location procedures. Currently, development is progressing on integrated procedures which are

evolutionary and probabilistic, using, for example, robust likelihood functions such as EDT and information from not-yet-triggered stations (*e.g.*, Horiuchi et al., 2005; Rydelek and Pujol, 2004; Satriano *et al.*, 2007ab; Cua and Heaton, 2007).

A current problem in direct-search location is how to describe in a standardized and compact way the sometimes topologically-complex location *pdf*. For example, such a description is needed if the *pdf* is to be included in standard earthquake catalogues and for rapid dissemination of probabilistic location information for earthquake early-warning. More generally, making full use of the extensive information in direct-search location solutions will require new methods and procedures to store, distribute and analyse the location *pdf*, maximum likelihood hypocentre, arrival residuals and weights, and other statistics and quality indicators of the solutions.

The continuing increase in computer speed will allow application of direct-search inversion methods to relative location of ensembles of events and for joint epicentral determination in the near future. The use of these methods will be important to explore more completely the vast solution space and better determine the error and resolution for such high-dimensional inverse problems.

The continuing increase in computer speed will also make practical earthquake location techniques using waveform recordings directly, without the intermediate stage of extracting phase arrival times. In these techniques, continuous waveform data streams are matched to synthetic Green's functions within a global-search over possible source locations and source parameters. This type of approach is used to locate previously unidentified earthquakes using low amplitude surface waves on off-line, continuous, broadband waveforms (Shearer, 1994; Ekstrom, 2006), and for automatic, real-time estimation of moment tensors and location from continuous broadband data streams (e.g., Kawakatsu, 1998). Waveform methods will likely be applied to earthquake location on local and regional scales as faster computers and more accurate 3D velocity models become available; related applications using simple ray or acoustic theories to generate the Green's functions show promising results (e.g., Baker et al., 2005).

VII. Bibliography

Books and Reviews

1. Aki K, Richards PG (1980) Quantitative Seismology, Freeman, New York.

2. Cerveny V (2001) Seismic Ray Theory. Cambridge University Press, Cambridge, UK.

3. Gasparini P, Gaetano, M, Jochen, Z (eds.) (2007) Earthquake Early Warning Systems, Springer, Berlin.

4. Goldberg DE (1989) Genetic Algorithms in Search, Optimization and Machine Learning, Addison-Wesley, Reading, MA.

5. Hammersley JM, Handscomb DC (1967) Monte Carlo Methods, Methuen, London.

6. Lee WHK, Stewart SW (1981) Principles and applications of microearthquake networks. Academic Press, New York.

7. Milne J (1886) Earthquakes and Other Earth Movements, Appelton, New York.

8. Reid, H. F. (1910). The Mechanics of the Earthquake, Vol. II of The California Earthquake of April 18, 1906, Report of the State Earthquake Investigation Commission, A.C. Lawson, Chairman, Carnegie Institution of Washington Publication 87 (reprinted 1969).

9. Press WH. Flannery BP, Saul AT, Vetterling WT (1992) *Numerical Recipes*, 2nd ed., Cambridge Univ. Press, New York.

10. Sambridge M, Mosegaard K (2002) Monte Carlo Methods In Geophysical Inverse Problems, *Rev. Geophys.*, 40:1009-1038

11. Sen M, Stoffa PL (1995) *Global optimization methods in geophysical inversion*, Elsevier, Amsterdam, 281p.

12. Sethian J A (1999) Level set methods and fast marching methods. Cambridge University Press, Cambridge, UK

13. Tarantola A (1987) Inverse problem theory: Methods for data fitting and model parameter estimation. Elsevier, Amsterdam.

14. Tarantola, A (2005). Inverse Problem Theory and Methods for Model Parameter Estimation. SIAM Philadephia.

15. Thurber CH, Rabinowitz N (eds.) (2000) Advances in Seismic Event Location, Kluwer, Amsterdam.

Primary Literature

16. Anderson K (1981) Epicentral location using arrival time order, *Bull. Seism. Soc. Am.*, 71:541-545.

17. Baker T, Granat R, Clayton RW (2005) Real-time Earthquake Location Using Kirchhoff Reconstruction, *Bull. Seism. Soc. Am.*, 95: 699–707.

18. Billings SD (1994) Simulated annealing for earthquake location, *Geophys. J. Int.*, 118:680-692.

19. Buland R (1976) The mechanics of locating earthquakes, Bull. Seism. Soc. Am., 66:173–187.

20. Calvert A, Gomez F, Seber D, Barazangi M, Jabour N, Ibenbrahim A, Demnati A (1997) An integrated geophysical investigation of recent seismicity in the Al-Hoceima region of North Morocco, *Bull. Seism. Soc. Am.*, 87:637-651.

21. Cua G, Heaton T (2007) The Virtual Seismologist (VS) Method: a Bayesian Approach to Earthquake Early Warning, in Gasparini P, Gaetano, M, Jochen, Z (eds.), Earthquake Early Warning Systems, Springer, Berlin.

22. Curtis A (1999a) Optimal experiment design: Cross-borehole tomographic examples, *Geophys. J. Int.*, 136:637-650.

23. Curtis A (1999b) Optimal design of focussed experiments and surveys, *Geophys. J. Int.*, 139:205-215.

24. Curtis A (2004a) Theory of model-based geophysical survey and experimental design Part A – Linear Problems, *The Leading Edge*, 23, No. 10: 997-1004.

25. Curtis A (2004b) Theory of model-based geophysical survey and experimental design Part B – Nonlinear Problems, *The Leading Edge*, 23, No. 10: 1112-1117.

26. Curtis A, Michelini A, Leslie D, Lomax A (2004) A deterministic algorithm for experimental design applied to tomographic and microseismic monitoring surveys, *Geophys. J. Int.*, 157:595–606.

27. Dreger D, Uhrhammer R, Pasyanos M, Frank, J, Romanowicz B (1998) Regional an far-regional earthqauke locations and source parameters using sparse broadband networks: A test on the

Ridgecrest sequence, *Bull. Seism. Soc. Am.*, 88:1353-1362.

28. Ekström G (2006) Global Detection and Location of Seismic Sources by Using Surface Waves, *Bull. Seism. Soc. Am.*, 96:1201-1212. doi: 10.1785/0120050175

29. Font Y, Kao H, Lallemand S, Liu C-S, Chiao L-Y, (2004) Hypocentral determination offshore Eastern Taiwan using the Maximum Intersection method. *Geophys. J. Int.,* 158:655-675.

30. Geiger L (1912) Probability method for the determination of earthquake epicenters from the arrival time only (translated from Geiger's 1910 German article), Bull. St. Louis University, 8:56-71.

31. Gentili S, Michelini A (2006) Automatic picking of P and S phases using a neural tree, Journal of Seismology, 10, 39-63. DOI: 10.1007/s10950-006-2296-6.

32. Horiuchi S, Negishi H, Abe K, Kamimura A, Fujinawa Y (2005) An Automatic Processing System for Broadcasting Earthquake Alarms, *Bull. Seism. Soc. Am.*, 95:708–718.

33. Husen S, Kissling E, Deichmann N, Wiemer S, Giardini D, Baer, M (2003) Probabilistic earthquake location in complex three-dimensional velocity models: Application to Switzerland, *J. Geophys. Res.*, 108: 2077-2102

34. Husen S, Smith RB (2004) Probabilistic Earthquake Relocation in Three-Dimensional Velocity Models for the Yellowstone National Park Region, Wyoming, *Bull. Seism. Soc. Am.*, 94:880–896.

35. Johnson C E, Lindh A, Hirshorn B (1994) Robust regional phase association*, U.S. Geol. Surv. Open-File Rept.* 94-621.

36. Kawakatsu H (1998) On the real-time monitoring of the long-period seismic wavefield, *Bull. Earthq. Res. Inst.*, 73, 267-274.

37. Kennett BLN (1992) Locating oceanic earthquakes – the influence of regional models and location criteria, *Geophys. J. Int.*, 108:848-854.

38. Kennett BLN (2006) Non-linear methods for event location in a global context, Phys. Earth Planet. Inter., 158:46-54.

39. Kirkpatrick S, Gelatt CD, Vecchi MP (1983) Optimization by simulated annealing, *Science*, 220:671-680.

40. Lahr JC (1999) HYPOELLIPSE: A Computer Program for Determining Local Earthquake Hypocentral Parameters,Magnitude, and First-Motion Pattern (Y2K Compliant Version) 1999 Version 1.0, *U. S. Geological Survey Open-File Report 99-23*, (On-Line Edition available at http://jclahr.com/science/software/hypoellipse/hypoel/hypoman/hypomst_pdf.pdf).

41. Lepage GP (1978) A new algorithm for adaptive multi-dimensional integration, J. Comput. Phys. 27:192–203.

42. Lomax A (2005) A Reanalysis of the Hypocentral Location and Related Observations for the Great 1906 California Earthquake, *Bull. Seism. Soc. Am.*, 91:861-877.

43. Lomax A (2008) Location of the Focus and Tectonics of the Focal Region of the California Earthquake of 18 April 1906, *Bull. Seism. Soc. Am.*, NN:nnn-nnn (accepted, in press).

44. Lomax A, Curtis A (2001) Fast, probabilistic earthquake location in 3D models using oct-tree importance sampling, *Geophys. Res. Abstr.* 3:955 (www.alomax.net/nlloc/octtree).

45. Lomax A, Virieux J, Volant P ,Berge C (2000) Probabilistic earthquake location in 3D and layered models: Introduction of a Metropolis-Gibbs method and comparison with linear locations, in

Advances in Seismic Event Location, Thurber CH, Rabinowitz N (eds.), Kluwer, Amsterdam.

46. Lomax A, Zollo A, Capuano P, Virieux J (2001), Precise, absolute earthquake location under Somma-Vesuvius volcano using a new 3D velocity model, *Geophys. J. Int.*, 146:313-331.

47. Maurer HR, Boerner DE (1998) Optimized and robust experimental design, *Geoph. J. Int.,* 132:458-468.

48. Moser TJ, van Eck T, Nolet G (1992a) Hypocenter determination in strongly heterogeneous earth models using the shortest path method, *J. Geophys. Res.*, 97:6563-6572.

49. Moser TJ, Nolet G, Snieder R (1992b) Ray bending revisited, *Bull. Seism. Soc. Am.*, 82:259–288.

50. Mosegaard K, Tarantola A (1995) Monte Carlo sampling of solutions to inverse problems, *J. Geophys. Res.*, 100:12431-12447.

51. Myers SC, Schultz CA (2000) Improving Sparse Network Seismic Location with Bayesian Kriging and Teleseismically Constrained Calibration Events, *Bull. Seism. Soc. Am.*, 90: 199–211.

52. Nicholson T, Gudmundsson Ó, Sambridge M (2004a) Constraints on earthquake epicentres independent of seismic velocity models, *Geophys. J. Int.*, 156:648-654

53. NicholsonT, Sambridge M, Gudmundsson Ó (2004b) Three-dimensional empirical traveltimes: construction and applications, *Geophys. J. Int.*, 156:307–328.

54. Podvin P, Lecomte I (1991) Finite difference computations of traveltimes in very contrasted velocity models: a massively parallel approach and its associated tools. *Geophys. J. Int.*, **105**:271-284.

55. Pujol J (2000). Joint event location - The JHD technique and applications to data from local seismic networks, in *Advances in Seismic Event Location*, Thurber CH, Rabinowitz N (eds.), Kluwer, Amsterdam.

56. Presti D, Troise C, De Natale G (2004) Probabilistic Location of Seismic Sequences in Heterogeneous Media, *Bull. Seism. Soc. Am.*, 94:2239–2253.

57. Rabinowitz N (2000) Hypocenter location using a constrained nonlinear simplex minimization method, in *Advances in Seismic Event Location*, Thurber CH, Rabinowitz N (eds.), Kluwer, Amsterdam.

58. Rabinowitz N, Steinberg DM (2000) A statistical outlook on the problem of seismic network configuration, in *Advances in Seismic Event Location*, Thurber CH, Rabinowitz N (eds.), Kluwer, Amsterdam.

59. Rawlinson N, Sambridge M (2004a) Wave front evolution in strongly heterogeneous layered media using the fast marching method *Geophys. J. Int.*, 156:631-647.

60. Rawlinson N, Sambridge M (2004b) Multiple reflection and transmission phases in complex layered media using a multistage fast marching method *Geophys.*, 69:1338–1350.

61. Rothman DH (1985) Nonlinear inversion, statistical mechanics, and residual statics estimation, *Geophysics*, 50:2784-2796.

62. Rydelek P, Pujol J (2004) Real-Time Seismic Warning with a Two-Station Subarray, *Bull. Seism. Soc. Am.*, 94:1546–1550.

63. Sambridge M (1998) Exploring multi-dimensional landscapes without a map, *Inverse Probl.*, 14:427–440.

64. Sambridge M (1999a) Geophysical inversion with a Neighbourhood algorithm, I, Searching a parameter space, *Geophys. J. Int.*, 138:479–494.

65. Sambridge M (1999b) Geophysical inversion with a neighbourhood algorithm, II, Appraising the ensemble, *Geophys. J. Int.*, 138:727–746,.

66. Sambridge M (2003) Nonlinear inversion by direct search using the neighbourhood algorithm, in *Intternational Handbook of Earthquake and Engineering Seismology*, 81B:1635-1637.

67. Sambridge M, Drijkoningen G (1992) Genetic algorithms in seismic waveform inversion, *Geophys. J. Int.*, 109:323-342.

68. Sambridge M, Gallagher K (1993) Earthquake hypocenter location using genetic algorithms, *Bull. Seism. Soc. Am.*, 83:1467-1491.

69. Sambridge M, Kennett BLN (1986) A novel method of hypocentre location, *Geophys. J. R. astr. Soc.*, 87:679-697.

70. Satriano C, Lomax A, Zollo A (2007a) Optimal, Real-time Earthquake Location for Early Warning, in Gasparini P, Gaetano, M, Jochen, Z (eds.), Earthquake Early Warning Systems, Springer, Berlin.

71. Satriano C, Lomax A, Zollo A (2007b) Real-time evolutionary earthquake location for seismic early warning, *Bull. Seism. Soc. Am.*, NN:nnn-nnn. (in revision)

72. Shearer, P. M. (1994) Global seismic event detection using a matched filter on long-period seismograms, *J. Geophys. Res.* 99:13,713–13,735.

73. Shearer PM (1997) Improving local earthquake locations using the L1 norm and waveform cross correlation: Application to the Whittier Narrows, California, aftershock sequence., *J. Geophys. Res.* 102:8269-8283.

74. Steinberg, DM, Rabinowitz N, Shimshoni Y, Mizrachi D (1995) Configuring a seismographic network for optimal monitoring of fault lines and multiple sources, *Bull. Seism. Soc. Am.* 85:1847-1857.

75. Stummer P, Maurer HR, Green AG (2004) Experimental Design: Electrical resistivity data sets that provide optimum subsurface information, *Geophysics*, 69:120-139.

76. Tarantola A, Valette B (1982) Inverse problems = quest for information, *J. Geophys. Res.* 50:159-170.

77. Thurber CH, Kissling E (2000) Advances in travel-time calculations for three-dimensional strucutres, in *Advances in Seismic Event Location*, Thurber CH, Rabinowitz N (eds.), Kluwer, Amsterdam.

78. Uhrhammer RA (1980) Analysis of small seismographic station networks, *Bull. Seism. Soc. Am.*, **70**:1369-1379.

79. Um J, Thurber C (1987) A fast algorithm for two-point seismic ray tracing, *Bull. Seism. Soc. Am.*, 77:972-986.

80. van den Berg J, Curtis A, Trampert, J. (2003) Bayesian, nonlinear experimental design applied to simple, geophysical examples. *Geophys. J. Int.*, 55(2):411-421. Erratum: (2005) *Geophys. J. Int.*, 161(2):265.

81. Vidale JE (1988) Finite-difference calculation of travel times. *Bull. Seism. Soc. Am.*, **78**:2062-2078.

82. Winterfors E, Curtis A (2007) Survey and experimental design for nonlinear problems. *Inverse Problems*, submitted.

83. Withers M, Aster R, Young C, Beiriger J, Harris M, Moore S, Trujillo J, (1998), A comparison of select trigger algorithms for automated global seismic phase and event detection, *Bull. Seism. Soc. Am.*, 88:95–106.

84. Wittlinger G, Herquel, G, Nakache T (1993) Earthquake location in strongly heterogeneous media, *Geophys. J. Int.*, 115:759-777.

85. Zhou H (1994). Rapid 3-D hypocentral determination using a master station method, *J. Geophys., Res.*, 99:15439-15455.

		Example	Lat (°)	Lon (°)	Depth (km)	rms (s)	gap (°)	Δ_0 (km)	N_P	$Vpdf$ (km³)	R_{pdf} (km)	l_{ell}^1 (km)	l_{ell}^2 (km)	l_{ell}^3 (km)
	ideal	1a	44.208	10.295	10.98	0.399	89	9.1	20	26	1.8	1.6	2.2	3.2
		1b	44.208	10.295	10.98	0.000	63	9.1	50	7	1.2	1.1	1.3	2.1
	few stations	2a	44.163	12.267	47.44	0.000	335	232	2	742001	82.3	30.9	53.9	223
		2b	44.172	9.565	77.60	0.001	192	25.8	4	21600	25.3	5.9	43.2	81.9
station distribution		2c	44.208	10.295	14.40	0.000	173	64.5	3	2011	7.8	4.8	7.3	20.2
		2d	44.208	10.295	10.98	0.000	99	9.1	8	66	2.5	2.1	2.7	4.9
	side	3	44.207	10.296	11.03	0.004	251	29.0	19	444	4.7	3.4	4.7	11.0
	far	4a	44.207	10.296	11.03	0.006	103	106	46	234	3.8	2.0	2.4	17.8
		4b	44.208	10.295	10.98	0.000	103	106	50	66	2.5	1.7	2.2	8.1
	experimental design	5a	44.215	10.290	15.13	0.014	229	9.9	6	1806	13.4	8.3	13.7	59.1
		5b	44.208	10.295	7.83	0.007	89	36.3	6	381	6.6	3.1	3.7	11.5
	L2-norm	6a	44.207	10.296	11.03	0.007	135	9.00	10	172	3.5	2.9	3.7	6.7
outlier		6b	44.120	10.267	9.02	0.813	156	10.5	10	172	3.5	3.0	4.2	9.0
	EDT	6c	44.221	10.305	9.94	0.006	132	9.4	10	167	3.4	4.5	7.7	15.2
		6d	44.215	10.304	10.02	0.540	133	9.0	10	275	4.0	10.7	30.8	42.9
	early warning	7a	44.139	10.194	24.79	0.012	307	15.6	3	628090	53.1	18.7	81.6	104
		7b	44.210	10.302	10.57	0.015	250	8.8	4	33908	20.1	18.4	30.0	105
		7c	44.208	10.295	11.12	0.008	227	9.1	5	1704	7.4	5.3	13.9	30.2
		7d	44.207	10.296	11.03	0.007	135	9.0	10	172	3.5	2.9	3.7	6.7
incorrect velocity model	L2-norm	8a	44.208	10.295	10.98	0.000	63	9.1	50	15	1.5	1.3	1.7	2.9
		8b	44.160	10.244	2.69	0.808	66	11.4	50	17	1.6	1.3	1.7	3.0
	EDT	8c	44.220	10.305	9.98	0.000	63	9.4	50	11	1.4	1.2	1.5	2.6
		8d	44.192	10.280	7.20	0.795	64	9.3	50	167	3.4	2.8	3.9	6.7

Table 1. Summary of results and quality indicators for the example locations. R_{pdf} is the radius of a sphere with volume V_{pdf}; l_{ell}^1, l_{ell}^2, l_{ell}^3 are the half-lengths of the error ellipsoid axes; N_P is the number of phases used for the location; Δ_0 is the distance to the closest station.

Figures

Figure 1
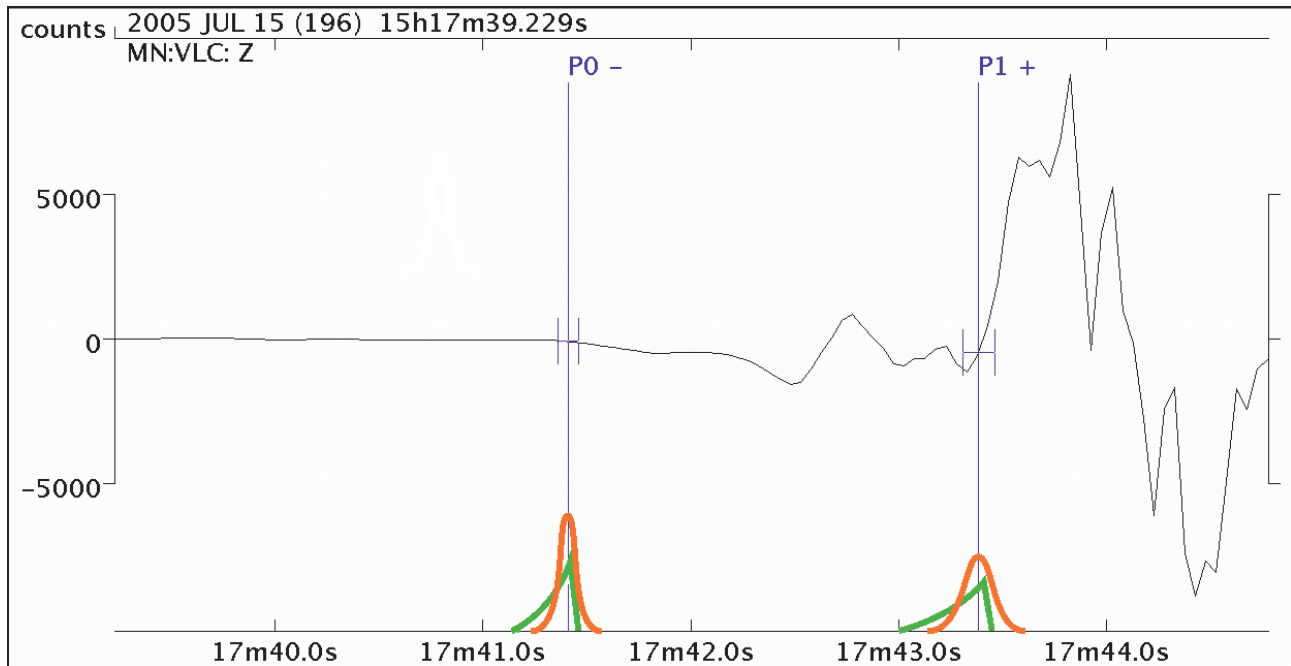
A short waveform segment (~5 sec) showing the first *P* wave arrivals from a small earthquake in Northern Italy recorded on a vertical component seismogram at a nearby station. Automatic arrival pick times (vertical blue lines) and uncertainty estimates (blue error-bars) are shown for two phases, a first arriving *P* phase (P0) and secondary *P* arrival (P1). The red curves show the data *pdf* functions representing these arrival pick times and uncertainties for an event location procedure where the data *P*(**d**) is approximated by a normal distribution. The green curves show irregular, asymmetric *pdf* functions that may more accurately represent the uncertainty in the phase arrival times; if such *pdf* functions were routinely estimated during arrival picking, they could be used without major difficulty for direct-search location.
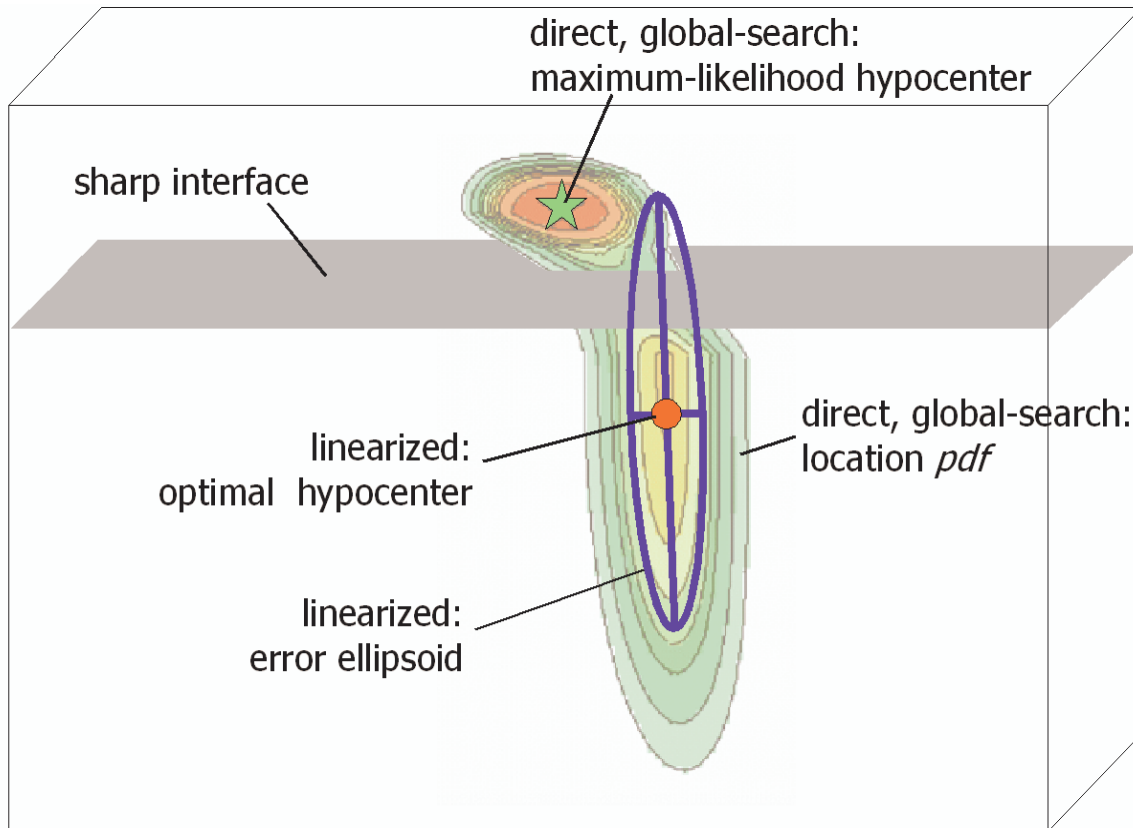
Figure 2

Schematic diagram comparing linearized and direct-search locations for the case where the complete location *pdf* is moderately complicated, with two maxima. This example arises from the case of a location at the limits of the recording network and near a sharp, horizontal interface in the velocity model between lower velocities above and higher velocities below. The coloured, contoured form shows the true location *pdf*, as should be determined by a complete, probabilistic, direct-search location procedure. A linearized location that iterates from an initial trial location below the sharp interface will find an optimal hypocenter near the secondary, local maximum of the location *pdf*, below the interface. The linearized error ellipsoid, based on the curvature of the misfit function at this optimal hypocenter, reflects the form of this secondary maximum only. The linearized location procedure never identifies or explores the primary maximum of the *pdf* above the sharp interface, and produces incorrect error information above this interface (i.e. the uppermost part of the error ellipsoid). A probabilistic, direct, global-search procedure can determine the complete location *pdf* and identify correctly the maximum likelihood hypocentre located above the sharp interface.

Figure 3

a)

b)

Example 1: An ideal location. a) Location obtained using the first 20, observed *P* or *S* arrival times; b) location obtained using the first 50, *P* or *S* corrected arrival times from the ideal, synthetic data set. The elements shown in these and the following figures are: stations used for location (blue dots, in
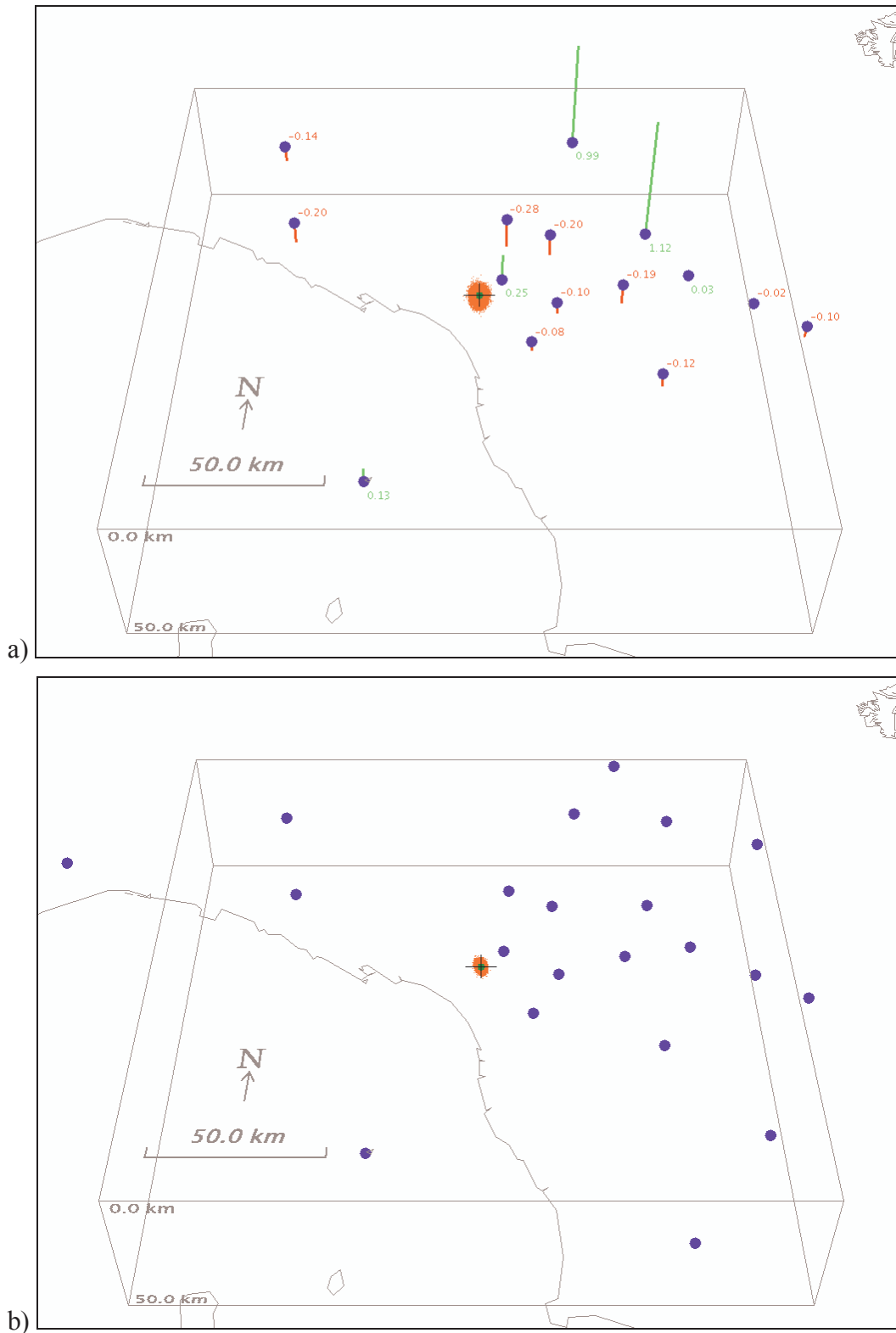
some cases stations fall outside the plotted region); location *pdf* (red cloud of points); maximum likelihood hypocenter (green dot); ideal, synthetic location (black cross); *P* arrival residuals at each station: positive (green, up-going bars) and negative (red, down-going bars), numbers indicate residual value in sec. The Hypoellipse linearized locations and ellipsoids do not differ significantly from the direct-search locations shown in this figure.

Figure 4

a)

b)
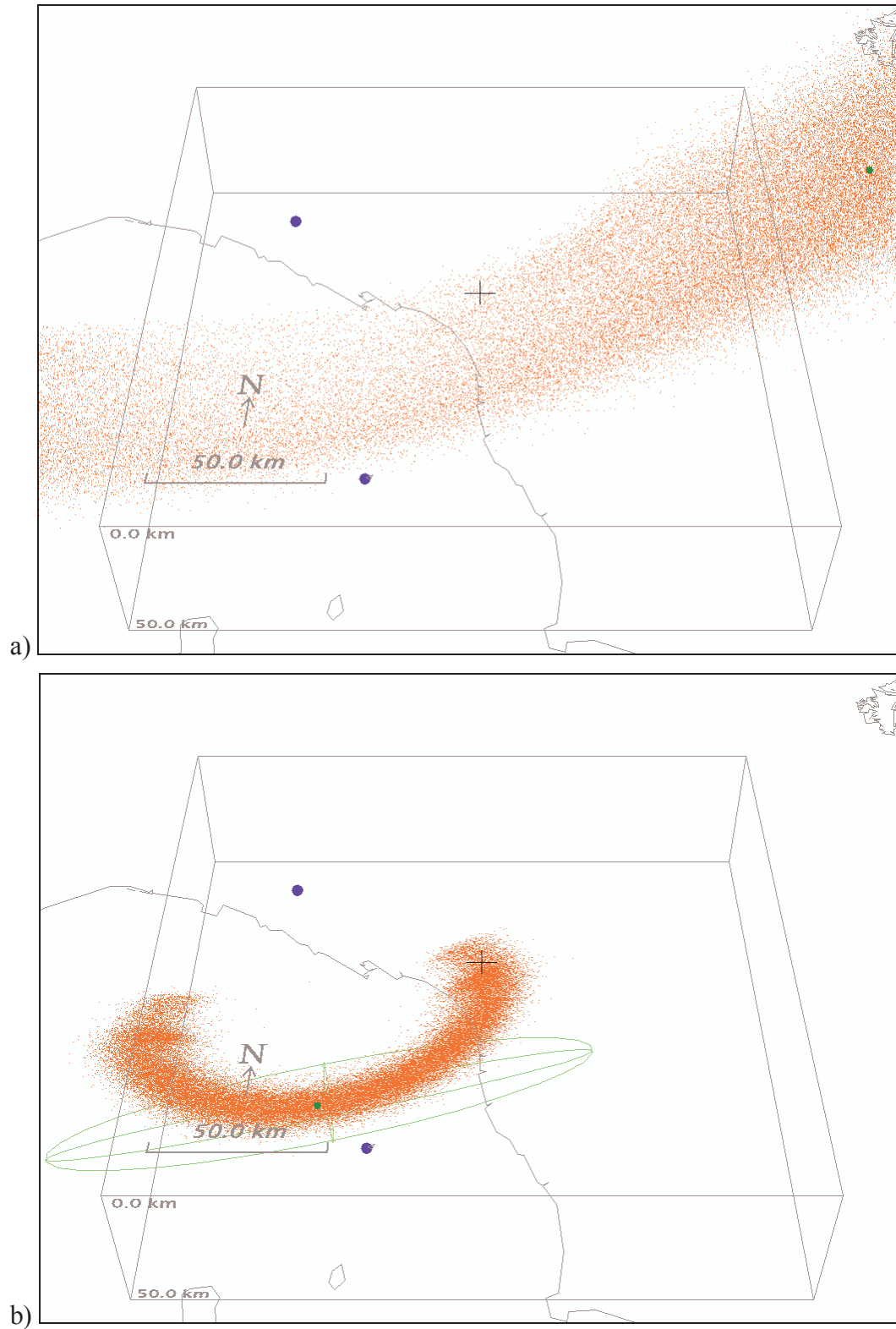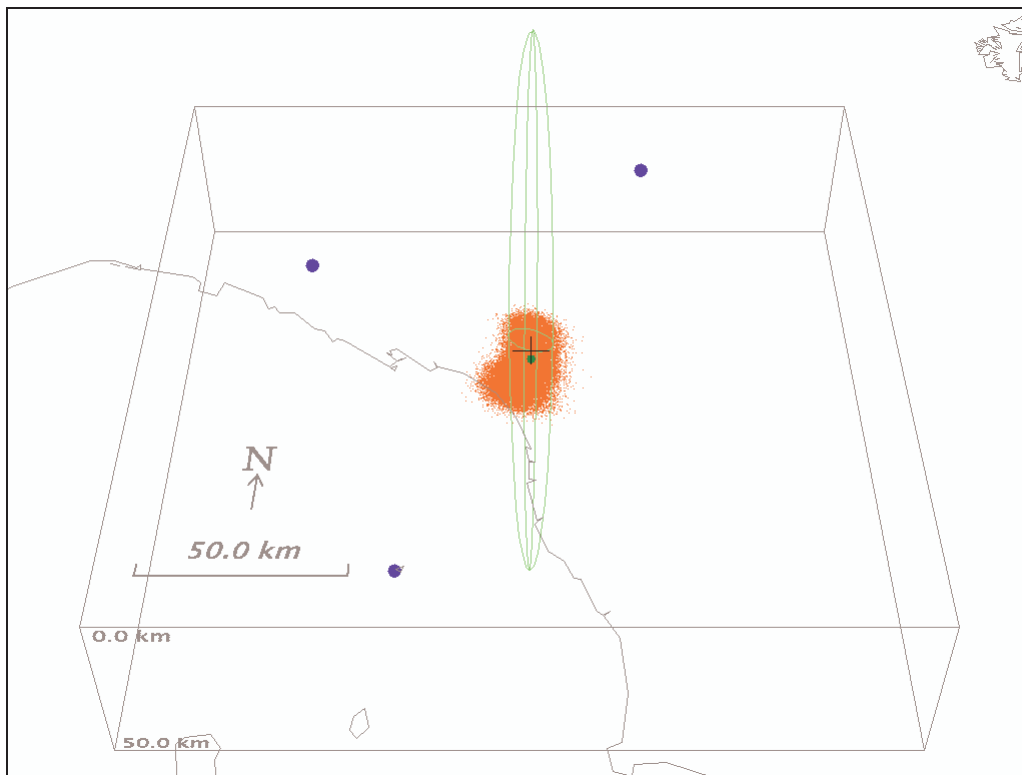
c)
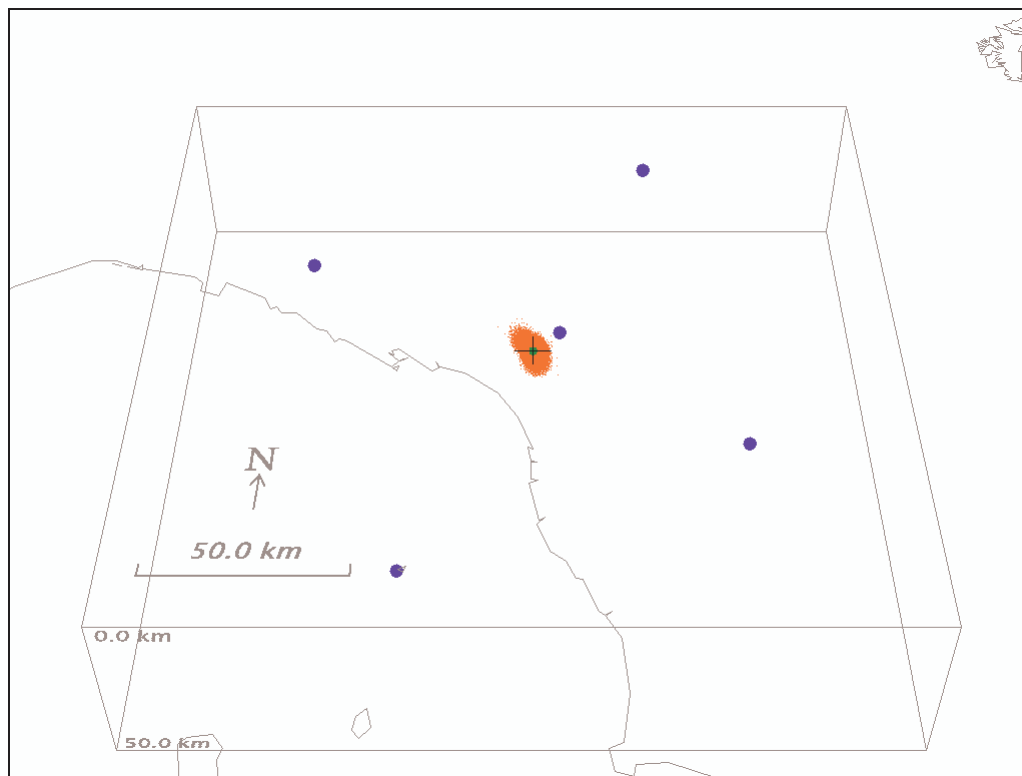
d)

Example 2: Few available stations. Locations obtained using progressively (a-d) a larger number of arrival observations. a) 2P phases (2 stations); b) 2P and 2 *S* phases (2 stations); c) 3P phases (3 stations); d) 5P and 3S phases (5 stations). For the locations in a) and b) the oct-tree search is performed to 100 km depth. In this and the following figures the 68% Hypoellipse ellipsoid is shown with green lines. Hypoellipse linearized location: does not converge for the location in panel a); ellipsoid differs markedly from the direct-search location *pdf* in panels b) and c); and does not differ

markedly from the direct-search location in panel d).

Figure 5
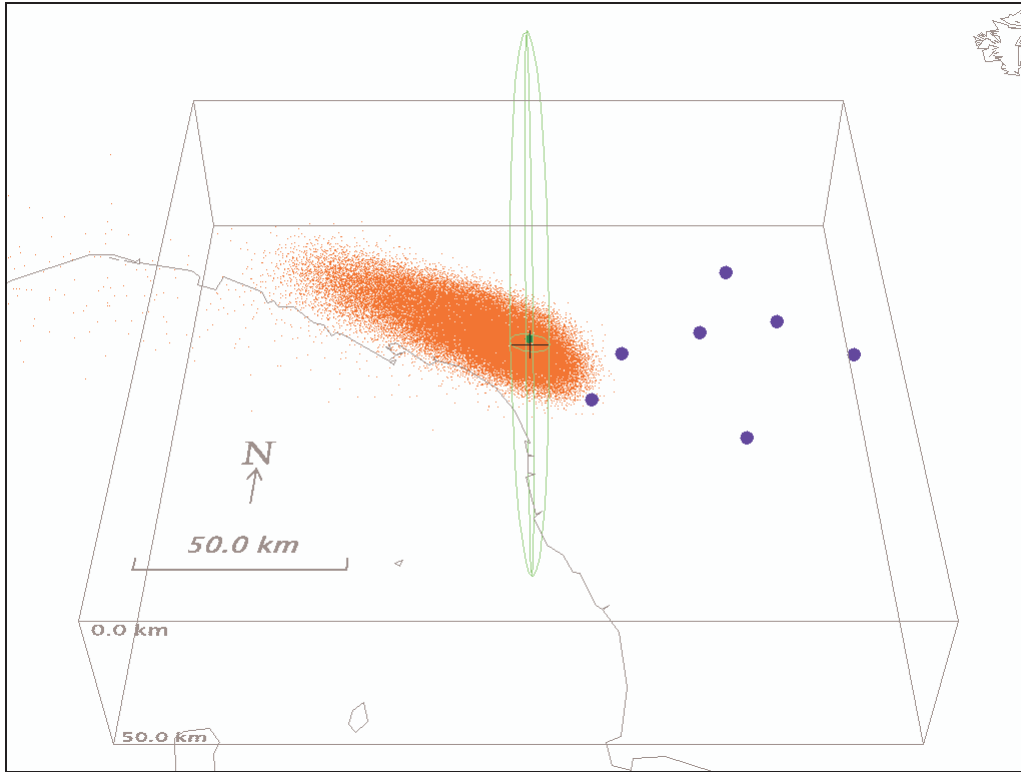
Example 3: Stations to one side of the event. A location example with *P*-wave arrival times at 7 stations only to the southeast of the event. The Hypoellipse ellipsoid differs markedly from the direct-search location *pdf* in this figure.

Figure 6

a)

b)
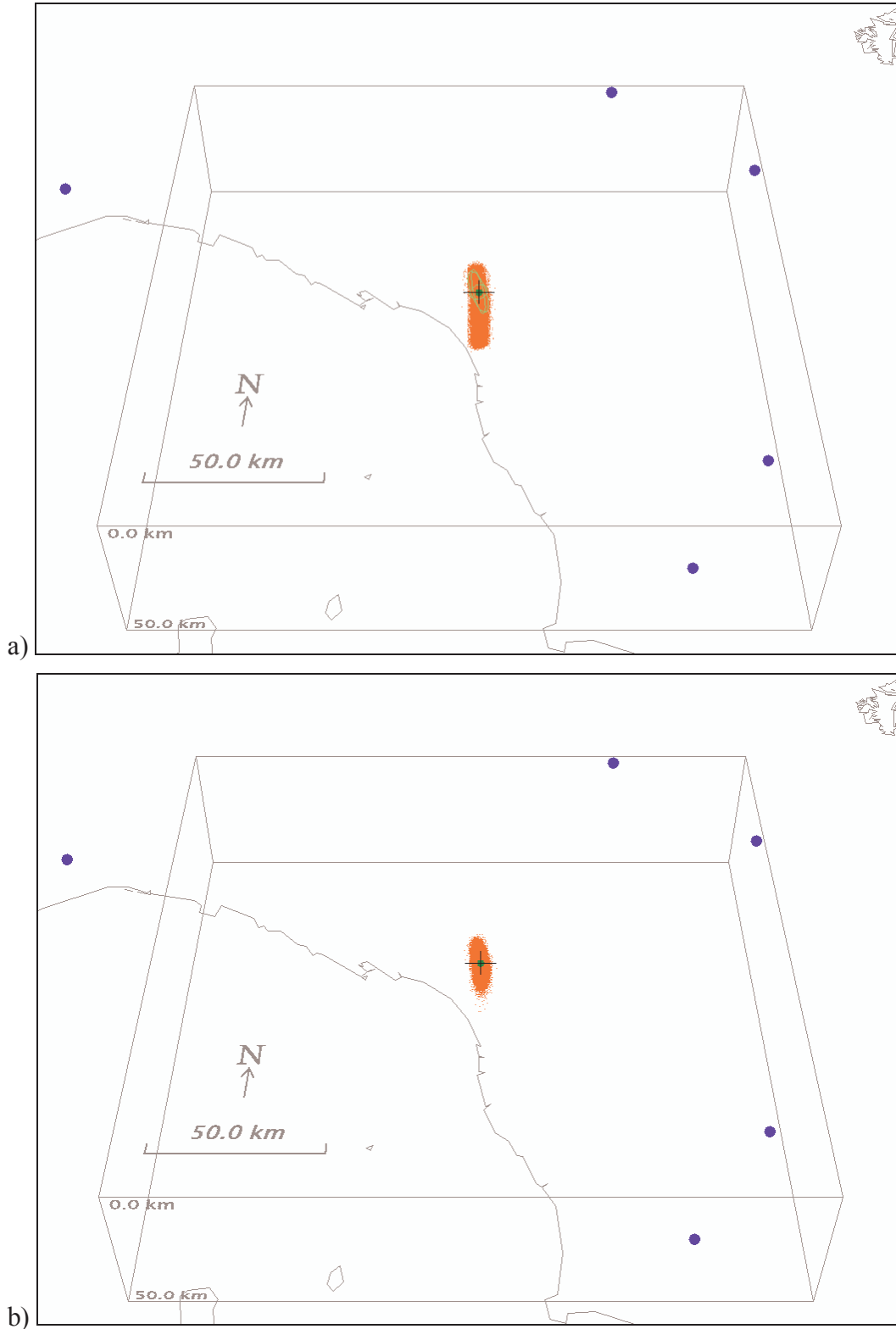
Example 4: Stations far from the event. A location example using stations far from the epicentre, with a) *P* arrival times only, b) both *P* and *S* arrival times. Hypoellipse linearized location: ellipsoid differs markedly from the direct-search location *pdf* in panel a); and does not differ markedly from the direct-search location in panel b).

Figure 7

a)

b)
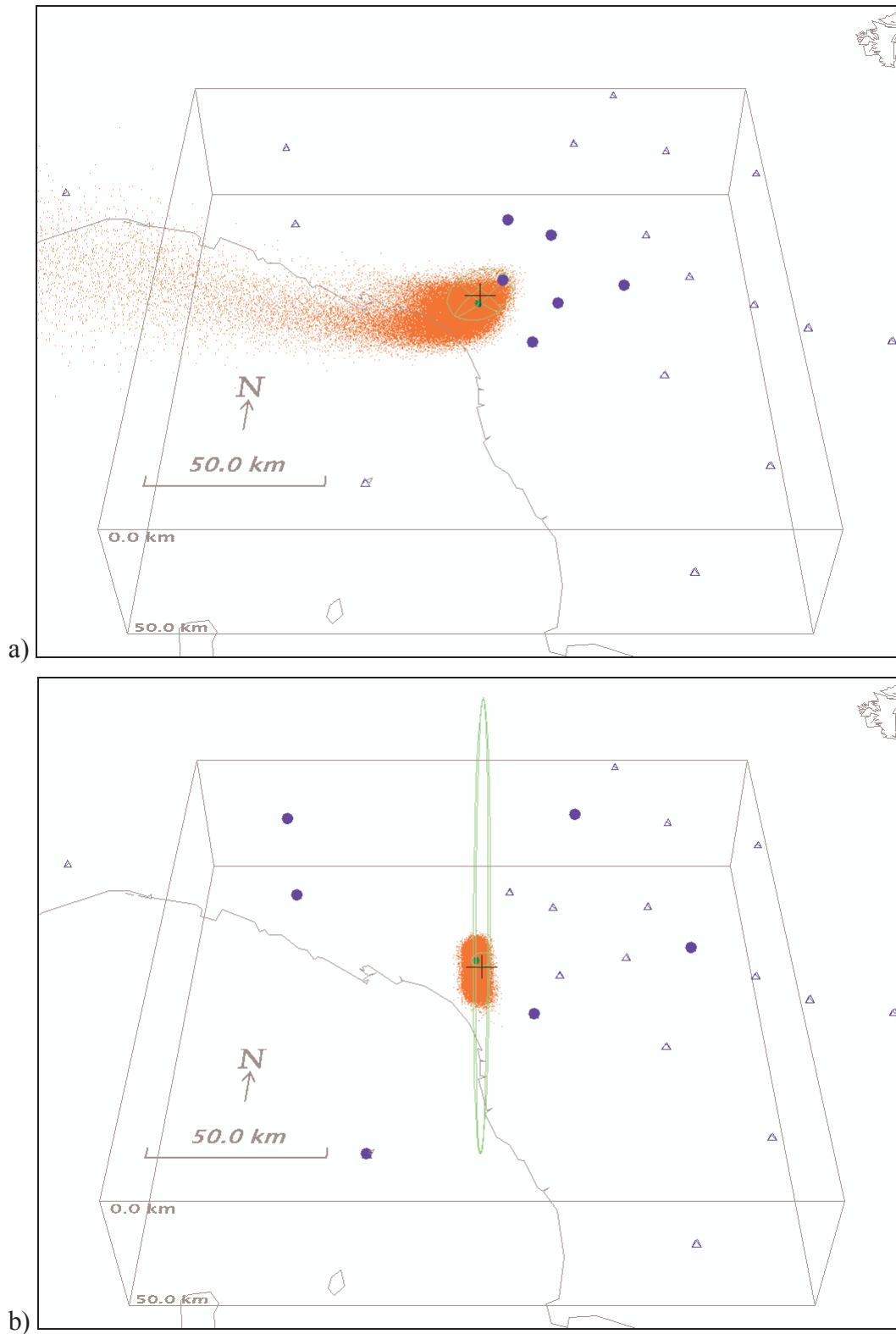
Example 5: Stations selection with experimental design. A location example showing a) Location using the stations with the first 6 available arrival times, b) location using an optimal set of 6 stations as

determined with a linearized experimental-design method. Available stations not used or selected are shown with open triangle symbols. Hypoellipse linearized location: ellipsoids differ markedly from the direct-search location *pdf* 's in panels a) and b).

Figure 8

a)

b)
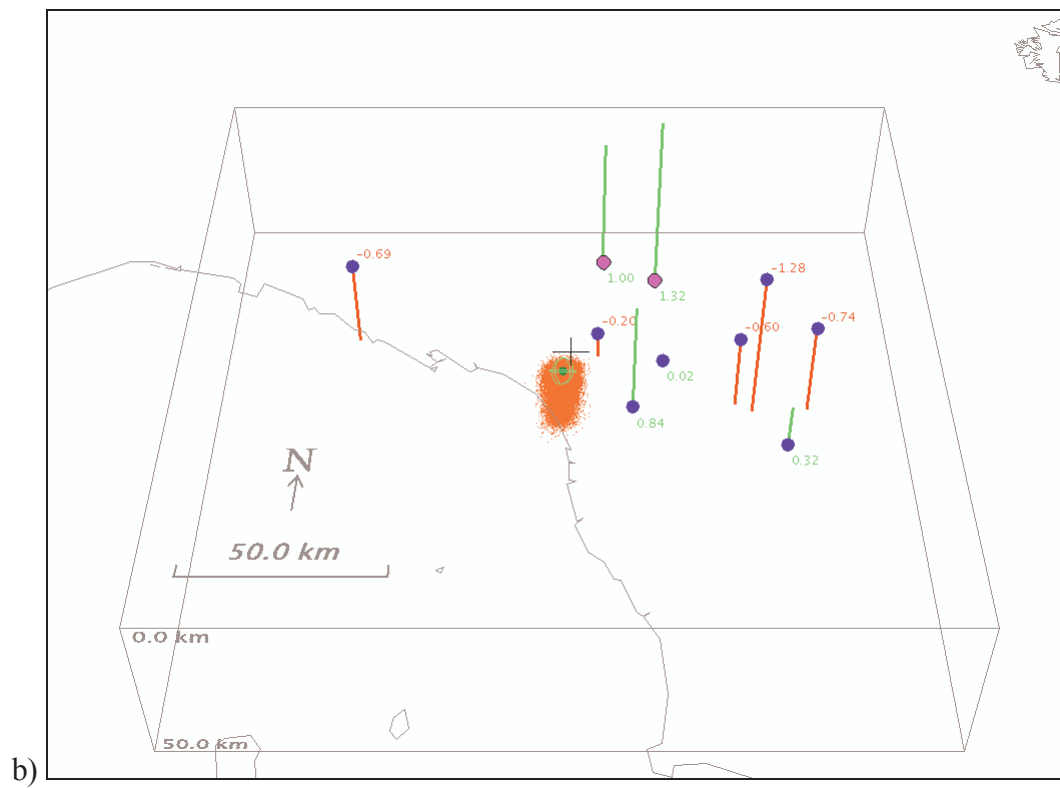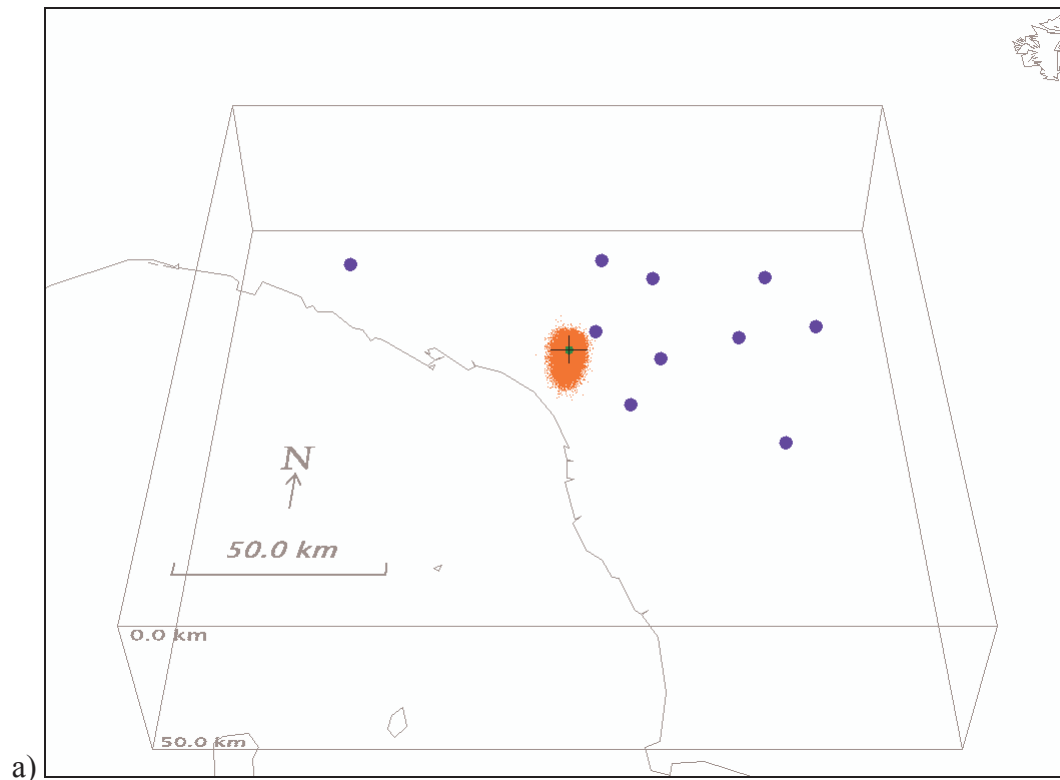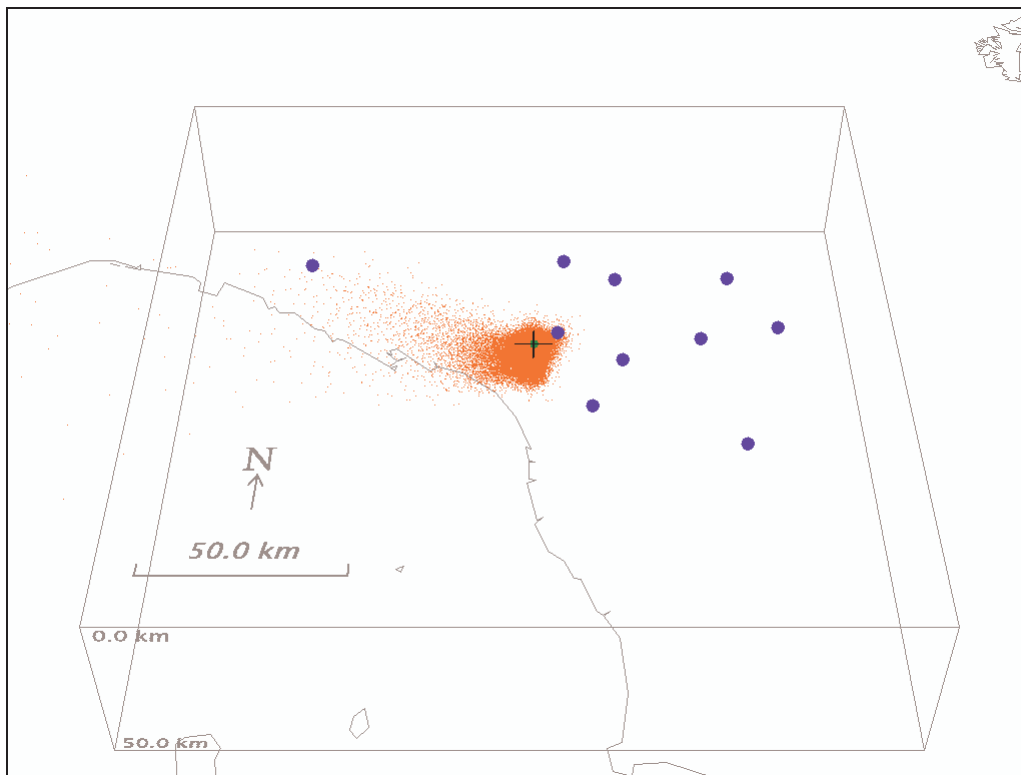
c)
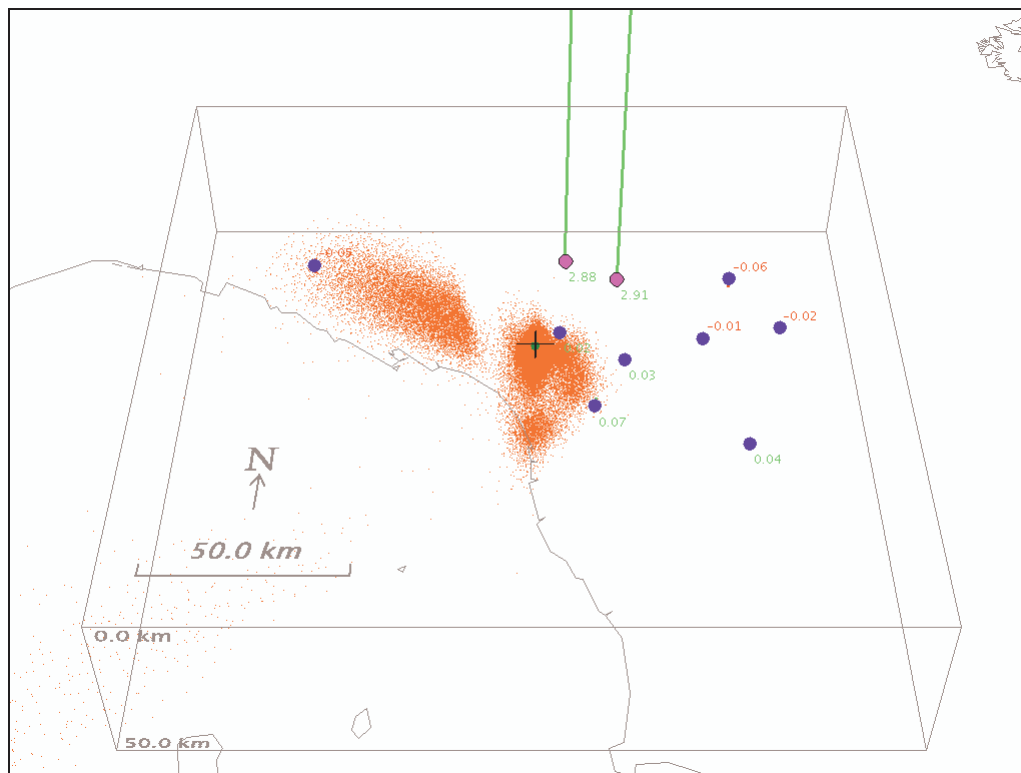
d)

Example 6: Incorrect picks and phase identification - outlier data. Locations using ten *P*-wave arrival times with L2-norm and a) no outliers, b) two arrival-time outliers, and with EDT and c) no outliers, d) two arrival-time outliers. The stations with outlier arrivals are shown with violet dots. Note the small *pdf* of L2-norm regardless of the outliers and, in contrast, the ability of EDT to detect the

outliers (see text). The Hypoellipse ellipsoid differs markedly from the direct-search location *pdf* in panel b). Hypoellipse not compared to EDT locations in panels c) and d).

Figure 9

a)

b)

c)

d)
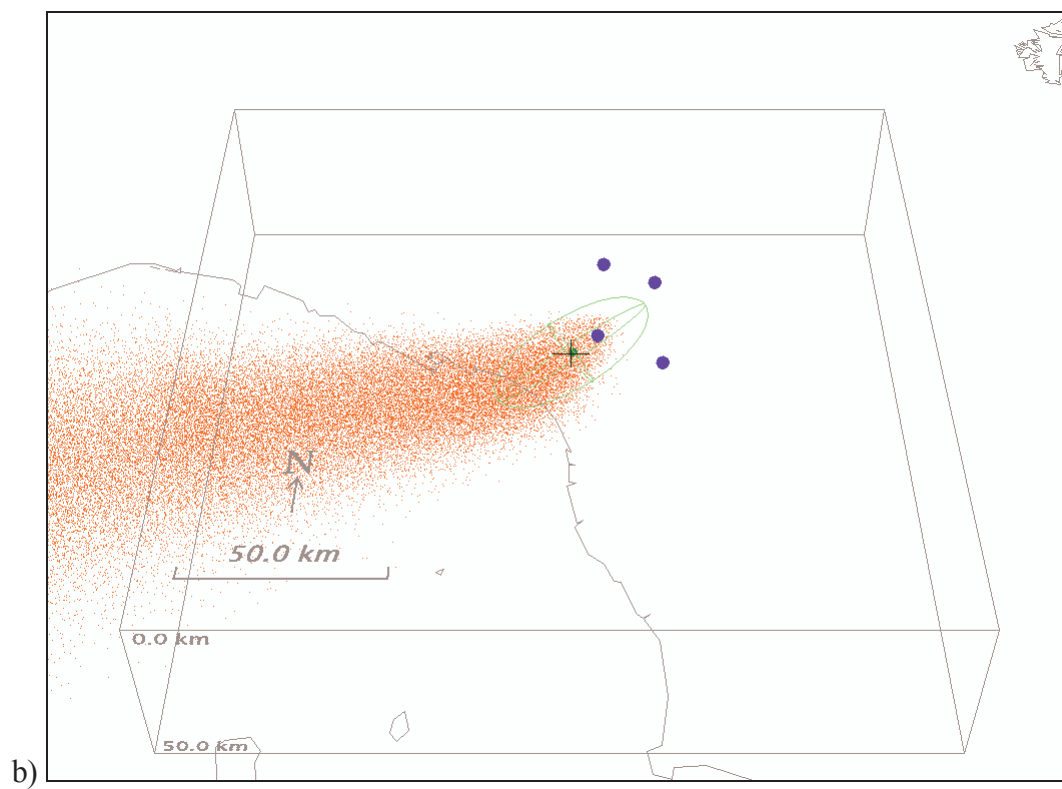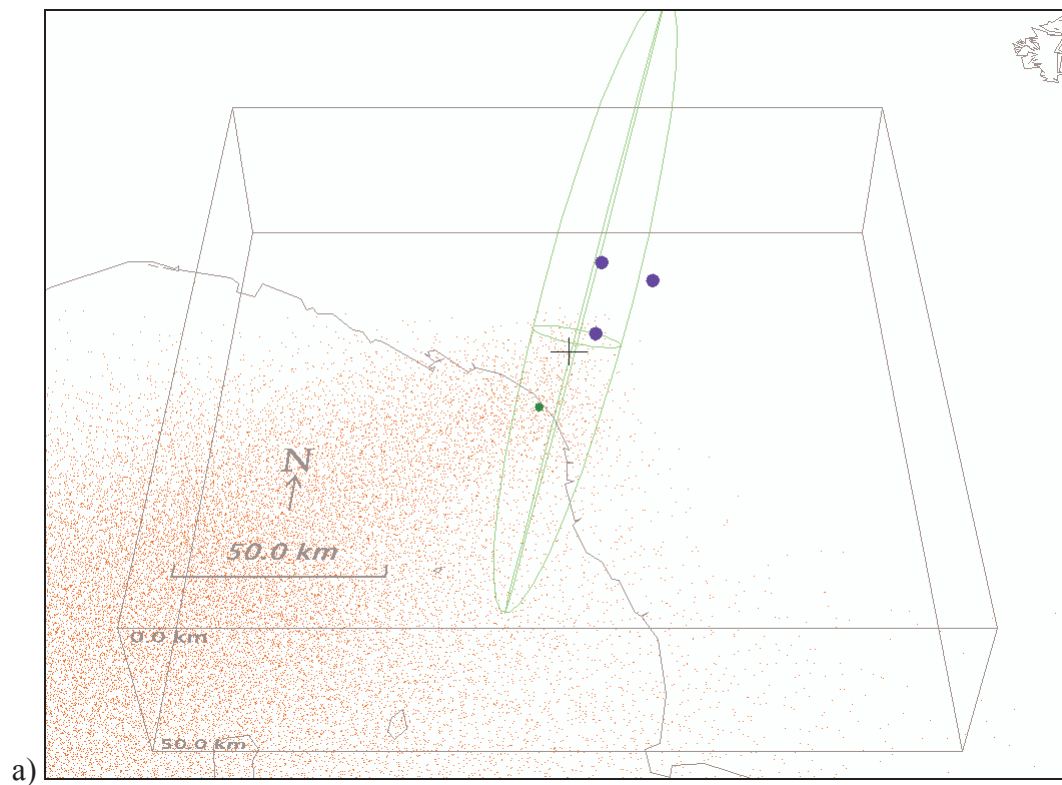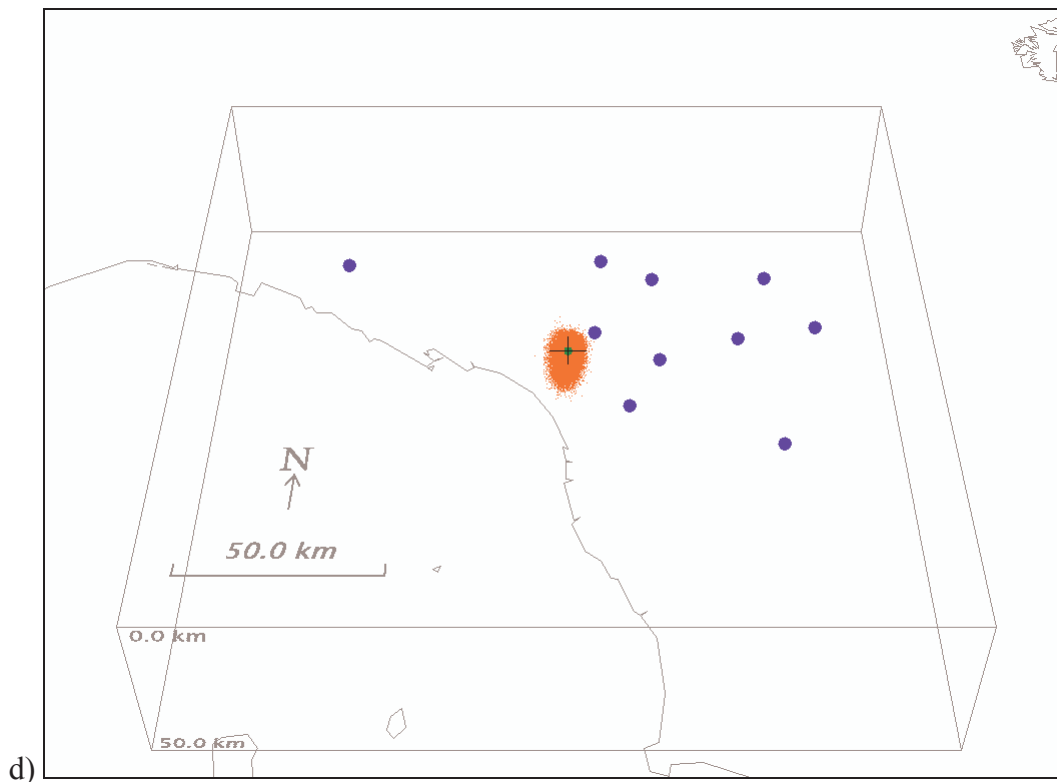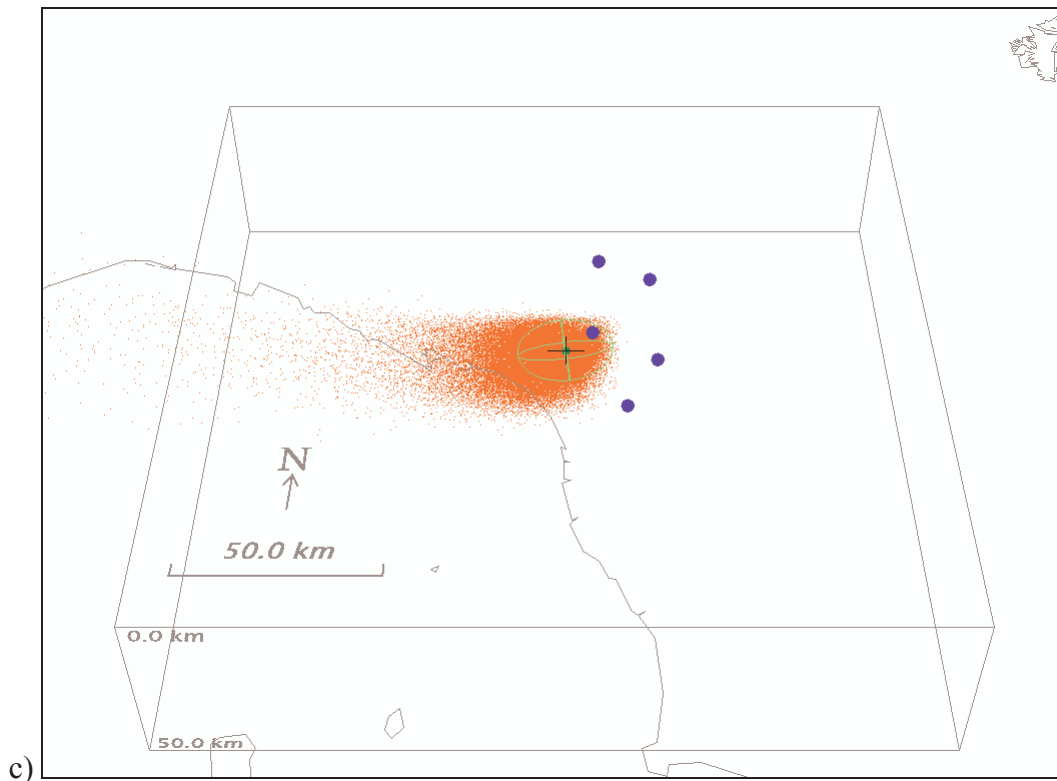
Example 7: Earthquake early-warning scenario. Progressive location using a) 3, b) 4, c) 5 and d) 10 stations. Hypoellipse linearized location: ellipsoids differs markedly from the direct-search location *pdf*'s in panel a), b) and c); and does not differ markedly from the direct-search location in panel d).

Figure 10

a)

b)
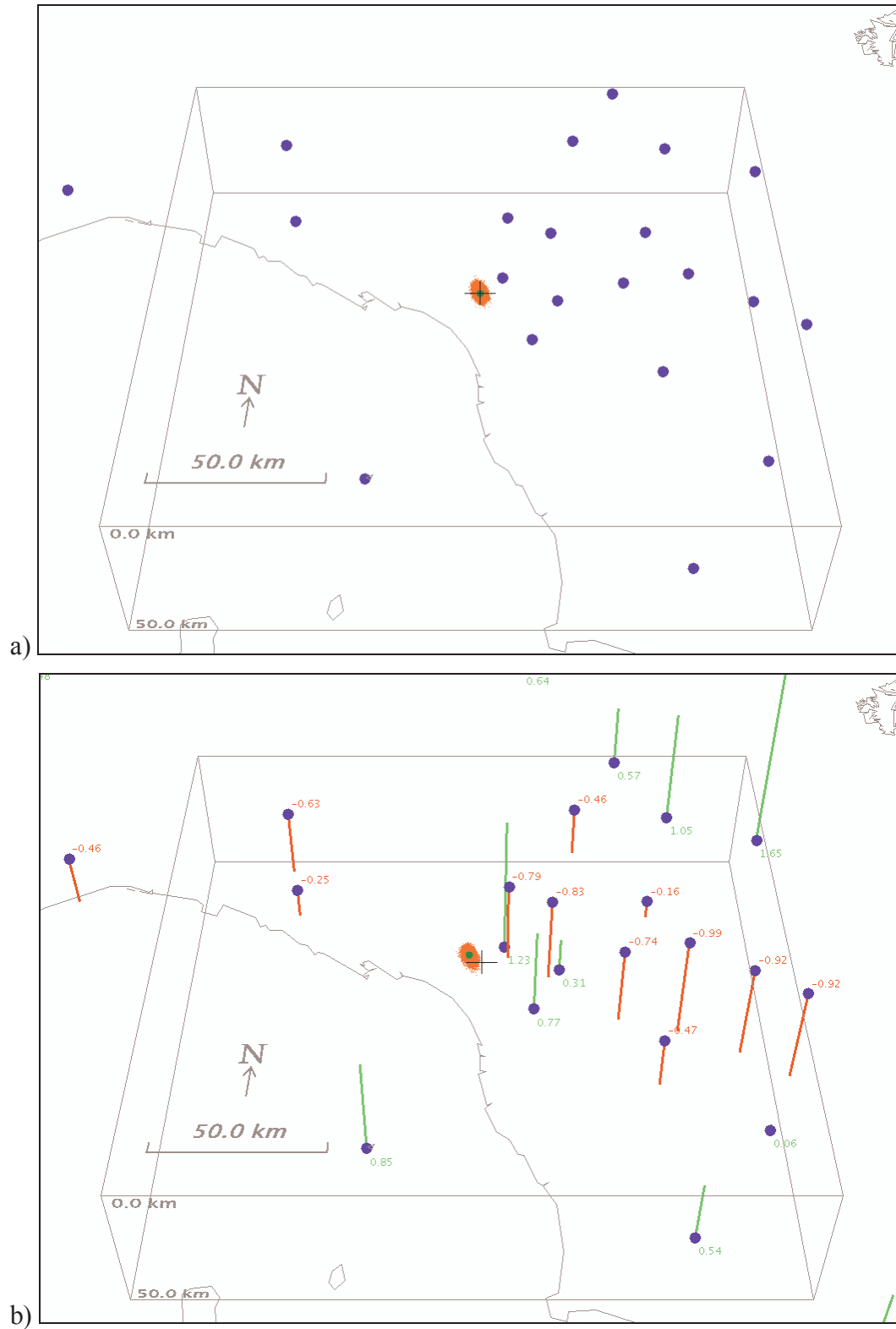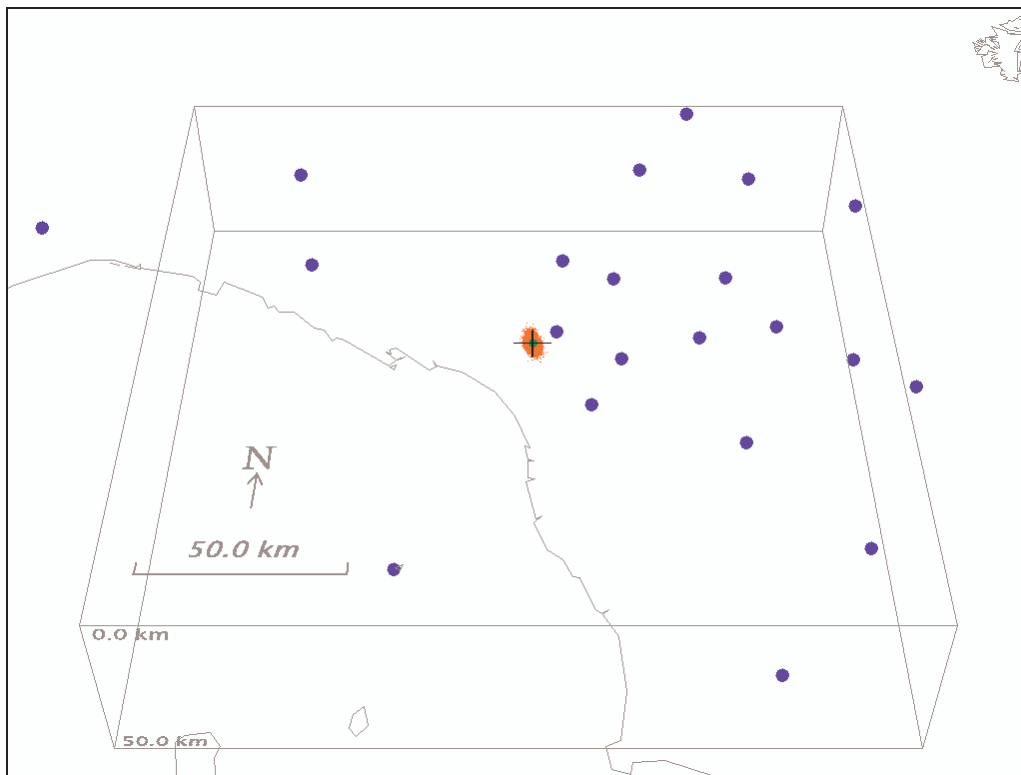
c)
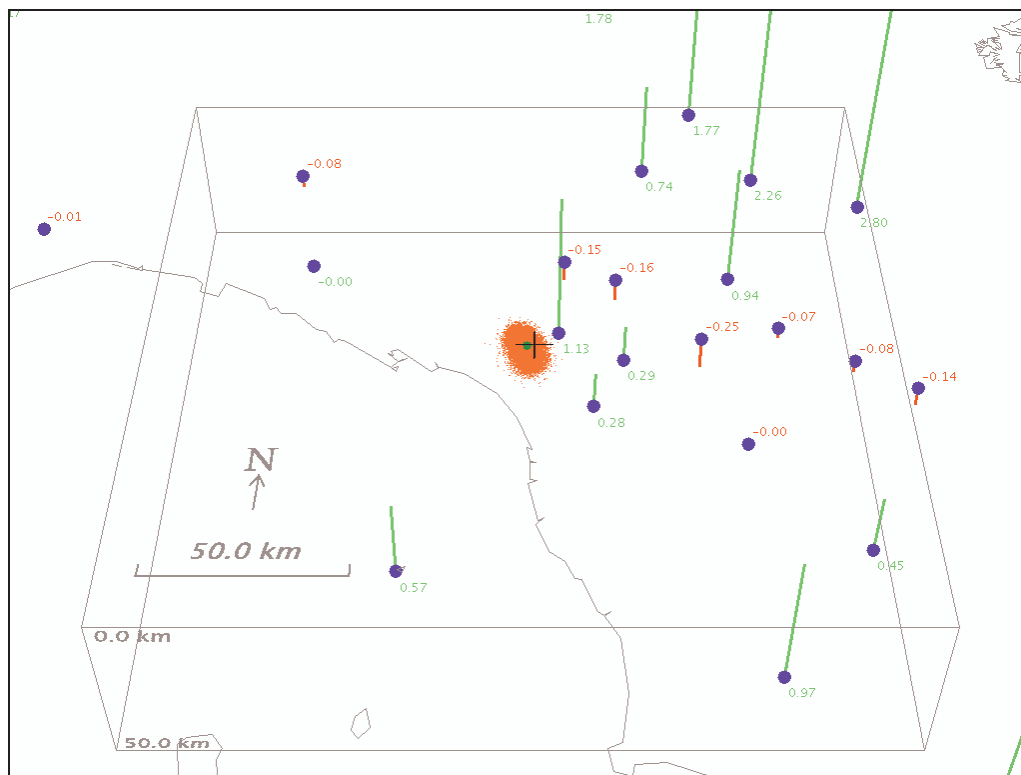
d)

Example 8: Incorrect velocity model. Locations using 50 *P* arrivals with the L2-norm and a) time corrections, b) no time corrections, and with EDT and c) time corrections, d) no time corrections. The locations without the ideal time corrections show the effect of an incorrect velocity model. The Hypoellipse linearized locations and ellipsoids do not differ markedly from the direct-search locations shown in this figure.